Elucidation of Therapeutic Potential of Caffeine Nanoparticles against Acute Myeloid Leukemia

Author

Usama Sabir

Registration Number

0000363902

Supervisor

Dr. Nosheen Fatima Rana

DEPARTMENT OF BIOMEDICAL ENGINEERING & SCIENCES

SCHOOL OF MECHANICAL & MANUFACTURING ENGINEERING

NATIONAL UNIVERSITY OF SCIENCES AND TECHNOLOGY

ISLAMABAD

2023

Elucidation of Therapeutic Potential of Caffeine Nanoparticles against Acute Myeloid Leukemia

Author

Usama Sabir

Registration Number

0000363902

A thesis submitted in partial fulfillment of the requirements for the degree of

MS Biomedical Sciences

Thesis Supervisor:

Dr. Nosheen Fatima Rana

Thesis Supervisor's Signature:

DEPARTMENT OF BIOMEDICAL ENGINEERING & SCIENCES

SCHOOL OF MECHANICAL & MANUFACTURING ENGINEERING

NATIONAL UNIVERSITY OF SCIENCES AND TECHNOLOGY,

ISLAMABAD

2023

THESIS ACCEPTANCE CERTIFICATE

Certified that final copy of MS/MPhil thesis written by **Regn No. 00000363902 Usama Sabir** of **School of Mechanical & Manufacturing Engineering (SMME) (SMME)** has been vetted by undersigned, found complete in all respects as per NUST Statues/Regulations, is free of plagiarism, errors, and mistakes and is accepted as partial fulfillment for award of MS/MPhil degree. It is further certified that necessary amendments as pointed out by GEC members of the scholar have also been incorporated in the said thesis titled. **Elucidation of therapeutic potential of caffeine nanoparticles against Acute myeloid leukemia**

Signature: 

Name (Supervisor): Nosheen Fatima Rana

Date: 26 - Oct - 2023

Signature (HOD): 

Date: 26 - Oct - 2023

Signature (DEAN): 

Date: 26 - Oct - 2023

Declaration

I certify that this research work titled **Elucidation of Therapeutic Potential of Caffeine Nanoparticles against Acute Myeloid Leukemia** is my own work. The work has not been presented elsewhere for assessment. The material that has been used from other sources has been properly acknowledged/referred to.

Signature of Student

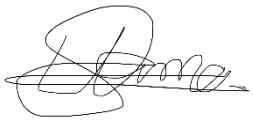

Usama Sabir

2021-NUST-MS-BMS-363902

Copyright Statement

Acknowledgements

I am thankful to my Creator Allah Subhana-Watala to have guided me throughout this work at every step and for every new thought which You setup in my mind to improve it. Indeed, I could have done nothing without Your priceless help and guidance. Whosoever helped me throughout the course of my thesis, whether my parents or any other individual was Your will, soindeed none be worthy of praise but You.

I am profusely thankful to my beloved parents who raised me when I was not capable of walking and continued to support me throughout in every department of my life.

I would also like to express special thanks to my supervisor Dr. Nosheen Fatima Rana forher help throughout my thesis and also for the Nano and Micro Drug Delivery course which she has taught me. That course was the motivation behind this research work.

I would also like to pay special thanks to Nimra Idrees, Urooba Tariq, Sahar Fatima, Laiba Hareem and Osama Khan for their tremendous support and cooperation. Each time I got stuck in something; they came up with the solution. Without their help, I wouldn't have been able to complete my thesis. I appreciate their patience and guidance throughout the whole thesis.

I would also like to thank Dr. Asim Waris, Dr. Aneeqa Noor and Dr. Mehak Rafiq for being on my thesis guidance and evaluation committee. I am also thankful to my senior TehreemTanveer for her support and cooperation.

Finally, I would like to express my gratitude to all the individuals who have rendered valuable assistance to my study.

Table of Contents

Table of Figures

List of Tables

Table of Abbreviations

AML	Acute Myeloid Leukemia
IARC	International Agency for Research on Cancer
DOX	Doxorubicin
FITU	Ferrocene-Incorporated Thiourea
ALL	Acute Lymphoblastic Leukemia
CLL	Chronic Lymphocytic Leukemia
CML	Chronic Myelogenous Leukemia
Np	Nanoparticles
UV-Vis spectroscopy	Ultraviolet–visible spectroscopy
XRD	X-ray Diffraction
FTIR	Fourier Transform Infrared
EDX	Energy Dispersive X-Ray Analysis
SEM	Scanning Electron Microscopy
ER	Estrogen Receptor
ROS	Reactive Oxygen Species
DMPC	1,2-Dimyristoyl-sn-glycero-3-phosphocholine
DPPC	Dipalmitoyl phosphatidyl choline
PEG	Polyethylene glycol

Abstract

Acute myeloid leukemia (AML) is a hematologic cancer characterized by defective differentiation of stem cells, leading to an overabundance of immature blood cells in the bone marrow and bloodstream. AML is a significant healthcare challenge that necessitates continuous patient management and the development of new therapeutic strategies. Benzene, a substance officially categorized as a group I carcinogen by the International Agency for Research on Cancer (IARC) since 1987, has been associated with the onset of AML and acute non-lymphocytic leukemia (ANL). Doxorubicin (DOX), a widely used chemotherapeutic agent, faces limitations in its clinical application due to its non-specific action and severe side effects like gonadotoxicity, cardiotoxicity, and nephrotoxicity, alongside issues with poor distribution and solubility. Caffeine also have short half-life. To address these issues, liposomal nanoparticles encapsulating caffeine and DOX separately were designed and synthesized to evaluate their therapeutic efficacy against benzene-induced AML in Wistar rats. Compared to free drugs, these nanoparticles aimed to enhance bioavailability and minimize adverse effects by enabling targeted delivery. Before proceeding with in vivo experiments, these nanoparticles were subjected to comprehensive in vitro characterization and assessment. The study's findings suggested that both caffeine and DOX, when delivered through liposomal nanoparticles, exhibited a more favorable profile, with reduced toxicity and improved drug distribution, offering a promising approach to AML treatment. Future research should continue to explore the intricacies of leukemia treatment and the nuanced effects of these drug-loaded nanoparticles. The pathways playing crucial role in AML could also be investigated against these nanoparticles formulation of caffeine.

Key Words: Acute Myeloid Leukemia (AML), Benzene Carcinogenicity, Doxorubicin Toxicity. Caffeine, Liposomal nanoparticles, Nanoparticle Efficacy

Chapter 1: Introduction

1.1 Cancer

Cancer is a lethal heterogeneous disease that is among the leading mortality causes across the globe. It is estimated that during 2020, new cases reported were 19.3 million and deaths filed were around 10 million s. Cancer is characterized by dysregulated cellular growth resulting in a mass proliferation of abnormal cells ultimately leading to tumor formation. Normal tissues ensure homeostasis between cell growth and death by controlling the cell cycle, but cancer cells become masters of their destiny by dysregulating the cell cycle. During cancer development, various genetic and epigenetic changes carry out the inactivation of tumor suppressor genes and the activation of oncogenes. Cancer involves the uncontrolled division of abnormal cells and their invasion into surrounding normal tissues and metastasis (Fares et al., 2020).

Various types of cancers have been categorized into broader groups, namely **carcinomas-** cancers originating from skin or tissue lining the organs, **sarcomas-** those arising from connective and supportive tissues; **lymphomas and myelomas-** the ones originating from cells involved in the immune system, and **leukemia** which is cancer originating from blood-forming cells. Another form is central nervous system cancer, which originates from cells of the brain and spinal cord (Boice *et al*., 1985).

1.1.1 The Process of Carcinogenesis

Cancer results from slow multistep mutations that might take decades to develop. Multiple factors are involved in cancer progression, including intrinsic and extrinsic factors contributing to cellular transformation (Wu *et al.,* 2016). Extrinsic factors are diet, lifestyle, environmental factors and carcinogens which cause DNA damage while intrinsic factors impart accumulation of mutations in genetic makeup. Intrinsic factors regulate the cell cycle, oxidative stress and pro-survival pathways

(Wu *et al.*, 2018). Cancer cells restrain metabolic pathways to fulfill energy requirements and unrestricted proliferation. Oncogenic mutations in neoplastic cells produce elevated ROS levels due to oncogenic signaling, mitochondrial dysfunction and increased metabolisms .

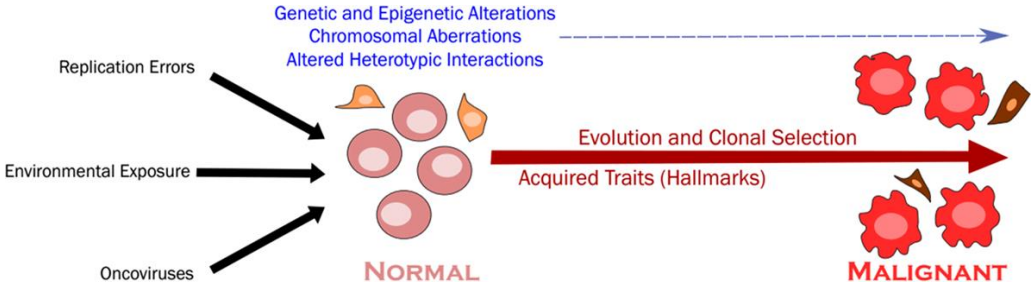

Figure 1 Causes of cancer (Fouad & Aanei, 2017

1.1.2 Hallmarks of Cancer

The hallmarks of cancer initially introduced in 2000 and revised in 2011 by Hanahan and Weinberg, are acquired characteristics due to which normal cells transform into malignant cells and lead to tumorigenesis. These hallmarks serve as a framework for understanding the intricacies of cancer. Cells achieve these biological competencies during cancer development, including sustaining proliferative signaling, activating invasion and metastasis, inducing angiogenesis, acquiring genome instability, evading growth suppressors, enabling replicative telomeres, tumor-promoting inflammation, developing resistance to apoptosis and deregulating cellular energetics (Hanahan & Weinberg, 2011). Metastasis is the most lethal aspect of cancerous cells, achieved by Endothelial Mesenchymal Transition (EMT). They metastasize by detaching from the primary tumor and invading the circulatory and lymphatic system, thereby escaping the immune system and increasing in different organs or tissues. These uncontrolled masses of tumor cells can migrate and spread to other body organs (Suhail et al., 2019), interact with stromal cells to generate a microenvironment that promotes cancer cell survival. Cancer cells escape from immune destruction by immunomodulation which involves various

traits acquired or lost by cancer cells, for example, the release of immuno-suppressants or deletion of tumor-specific antigens respectively (Fouad & Aanei, 2017).

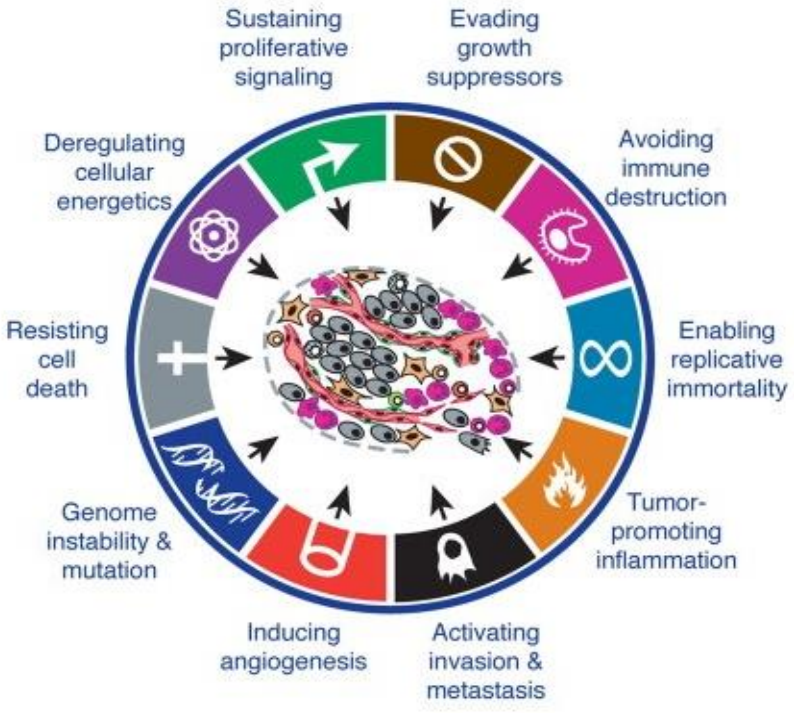

Figure 2 Hallmarks of cancer (Hanahan & Weinberg, 2011)

Cell cycle checkpoints make sure to destroy abnormal cells by apoptosis. Still, cancer cells do not replicate under the cell cycle regulation, thereby escaping from apoptosis by functional loss of checkpoints leading to generic instability. Protooncogenes perform the normal cell growth and division function, but after acquiring genetic mutations, they become oncogenic . Besides this, cancer stem cells achieve immortality due to alternative telomere lengthening. Altered genetics and epigenetic mutations also lead to angiogenesis due to elevated expression of VEGF (Caon et al., 2020).

1.1.3 Cancer Progression Levels

Many cellular processes contribute to the emergence of neoplasm and malignant cell progression. Mutations have identified different stages of cancer in other genes involved in various metabolic pathways. Normal cells first change into the hyperplastic stage, then transform into the dysplastic phase, indicated by an increase in nuclear to cytoplasmic content. These dysplastic cells further transit to the neoplastic stage before acquiring metastatic properties (Hassanpour & Dehghani, 2017).

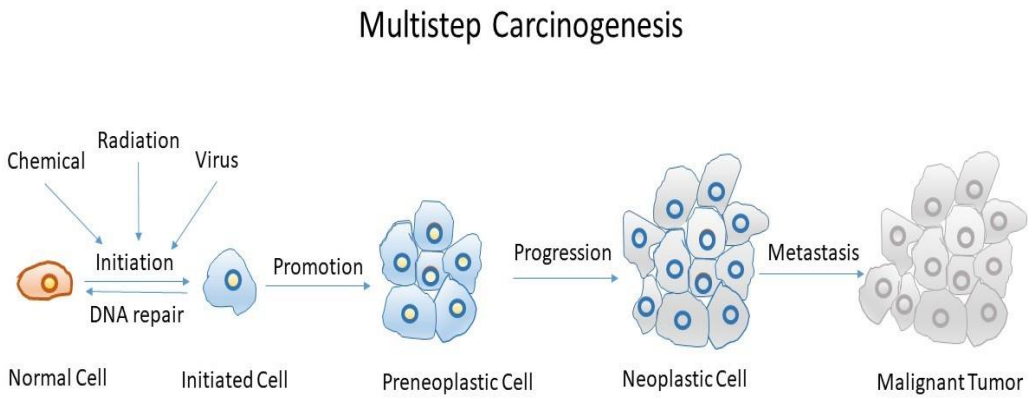

Figure 3 Levels of cancer progression

1.2 Leukemia

Leukemia is a hematological malignancy characterized by the overproduction of immature white blood cells (WBCs) known as leucoblasts. These blast cells arise in blood and bone marrow, and infiltrate other body organs, such as the liver, spleen, lymph nodes, etc. The fate of hematopoietic stem cells is highly peculiar, specifically, their proliferation, differentiation, self-renewal and quiescence at the progenitor stage, but such hematologic hierarchy is not found in leukemic stem cells. Many vital elements such as interleukins, growth factors, hormones, transcription factors and many other regulating factors play critical role in the altered signaling (Sive & Göttgens, 2014).

Normal hematopoietic process is halted and malignant leukemic cells start to replace normal cells resulting in low production of red blood cells and platelets accompanied by an increase in atypical lymphocytes. Body immune system becomes defective due to decrease in normal leukocytes causing inability to fight against pathogens, slow blood clotting, thrombocytopenia, bleeding and anemia (Chopra & Bohlander, 2019).

Risk factors in leukemia progression are inherited or acquired via genetic mutations, chromosomal disorders, environmental factors such as exposure to ionizing radiations, carcinogens (benzene, alkylating agents) or previous therapies that pose an enhanced risk of leukemia (Behrmann et al., 2018).

1.2.1 Classification of Leukemia

Based on the cellular stage during hematopoiesis, leukemia is of two types, i.e., Acute Leukemia which is the uncontrolled proliferation of the undifferentiated cells involved in hematopoiesis and Chronic Leukemia defined as uncontrolled proliferation of the more differentiated but not fully mature or differentiated cells involved in hematopoiesis.

According to the French-American-British classification system, leukemia is divided into two main types: myeloid leukemia, distinguished by deregulated division of myeloid progenitor cells and lymphoblastic leukemia, which is deregulated division of lymphoid progenitor cells.

Both types of leukemia are further categorized into subcategories according to their morphology which depends on cell differentiation stage which fails to give next stage upon differentiation.

There are 3 types of lymphoblastic leukemia which include lymphoblastic leukemia with homogeneous structure L1, lymphoblastic leukemia with altered structure L2 and Burkitt's leukemia L3. This system of classification is based on the cell morphology involved in hematopoiesis (Ladines-Castro et al., 2016).

If differentiation or maturation is blocked at myeloid stem cell and they continue to proliferate exponentially then this results in Acute Myeloid Leukemia (AML) but if maturation stops at myelocytic stage and they continue to proliferate, then this results in Chronic Myeloid Leukemia (CML). If differentiation to next stage gets blocked at promyelocyte stage, then it would result in Acute Promyeloid Leukemia (Sell, 2006).

Table 1 Classification and causes of leukemia

Classification	Causes of Leukemia and Symptoms	References
Acute Myeloid Leukemia	Genomic instability such as mutations in FLT3 and IL-3R genes in myeloid stem cells. Differentiation arrest results in immature blasts. ≥20% blast cells represent AML. Uncontrolled proliferation of immature myeloblasts by evading apoptosis. Alteration in bone marrow niche and immune system dysregulation.	(Behrmann *et al*., 2018) (Shallis *et al*., 2019)
Chronic Myeloid Leukemia	Reciprocal translocation of chromosome 9 and 22 results in Philadelphia chromosome formation. BCR-ABL1 fusion occurs. Tyrosine kinase proteins become constitutively active.	(McCafferty et al., 1990)

Acute Lymphoblastic Leukemia	Also known as childhood leukemia. heterogenous neoplasm at genetic level. Derived from B and T cells.	(Terwilliger & Abdul-Hay, 2017) (Hallek, Shanafelt, & Eichhorst, 2018
Chronic Lymphoblastic Leukemia	Heterogenous disease of mature clonal B cells. Expansion of CD5+ and CD25+ population in bone marrow and peripheral blood. Defective immune response.	(Hallek et al., 2018)

1.2.2 Diagnosis of AML

The diagnosis of AML is complicated because of its unique complex subtypes. Cancer can be treated successfully if diagnosed at early stages. AML is diagnosed by many ways, but blood tests are most common. Blood and bone marrow analysis are performed to differentiate leukemia (Döhner *et al*., 2017). Morphological analysis of blood and bone marrow is standard method for leukemia evaluation and therapy remission. Blood tests are performed for morphological analysis of myeloblast, bone marrow cells and peripheral blood cells because they show altered pattern in leukemia. The changes are increased cytoplasm to nucleus ratio, nuclear shape distortion and reduced cytoplasmic content. These properties reflect blast cells. If more than 20% blast cells are present in blood, then it is characterized as AML. Giemsa staining is considered as most preferable procedure for morphological analysis. AML can also be detected on basis of molecular markers and cytogenetics. Changes in renal

and hepatic biomarkers due to benzene cytotoxicity in serum are also used as key parameters for AML diagnosis (Blackburn *et al*., 2019).

1.2.3 Therapeutic Strategies of AML

Cancer survival rate declines due to diagnosis at late stage and lack of proper treatment on time. There are many conventional therapies to treat cancer more efficiently such as radiation therapy, chemotherapy, surgery, hormonal and immune therapy but numerous side effects are associated with them. One of the major challenges to overcome cancer is continuous emergence of drug resistance and non-specific target action.

Conventional therapies usually have high degree of toxic effects to normal cells and they also tend to damage vital organs. Chemotherapy has several adverse effects on normal cells because chemotherapeutic agents are incapable of distinguishing between normal and transformed cells (Singh *et al*., 2016). The major challenge in cancer therapy is cytotoxic and genotoxic effects of anti-cancer drugs on normal cells. In chemotherapy, anti-cancerous therapeutic agents are used to inhibit proliferation and induce cell death. Multidrug resistance (MDR) and adverse drug reactions (ADR) arise due to prolonged medication. Radiation and chemotherapies also cause severe side effects like vomiting, hair loss, fatigue, diarrhea, nausea, liver damage and neurological disorders during treatment (Schirrmacher, 2019). In addition to mentioned side-effects, targeted therapeutics and chemotherapy can also induce immunogenic cell death (Ahmed & Tait, 2020).

Allogenic or autologous stem cell transplantation is particularly used to treat AML. Doxorubicin, cisplatin, cytarabine are standard chemotherapeutic drugs used in AML eradication. Combination therapy with naturopathy has showed enhanced efficacy against AML. Some leukemic cells which survive chemotherapy can promote relapse of leukemia after successful treatment (Takami, 2018).

1.3 Benzene as Leukemogenic Agent

Benzene (molecular formula C6H12) is volatile, organic and aromatic hydrocarbon which exhibits high carcinogenic potency. The international agency for research on cancer has categorized benzene as a human carcinogen. It causes multiple alterations that lead to AML and other blood malignancies by multiple modes of action (Lu et al., 2020).

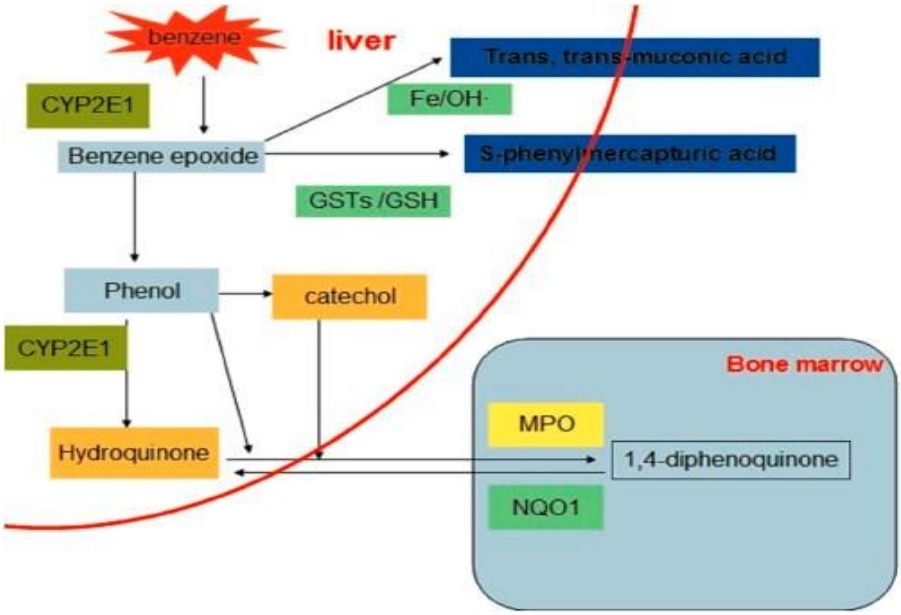

Figure 4 Metabolism of benzene into toxic metabolites (Han et al., 2018)

Benzene exerts its toxicity by breaking down into toxic metabolites i.e., phenol, benzene oxide, catechol, hydroquinone, trans-trans muconic acid. Cytochrome P450E1 (CYP) and E2 (CYP2E1 and CYP2F1/2A13) are mainly involved in oxidation of benzene into its metabolites (Peng & Ng, 2016).

Benzene is transformed into its toxic metabolites in liver and accumulate in bone marrow, directly or indirectly intensifying the mutations in normal cells resulting in alterations in hematopoietic signaling pathways which contribute to expansion of mutated cells . Its metabolites tend to interact

with genomic DNA leading to adduct formation, mismatch base pairing and chromosomal aberrations leading to dysregulated proliferation and apoptosis. Benzene metabolites also result in oxidative stress by increasing reactive oxygen species (ROS) levels which trigger DNA damage and mutations at genetic and epigenetic levels.

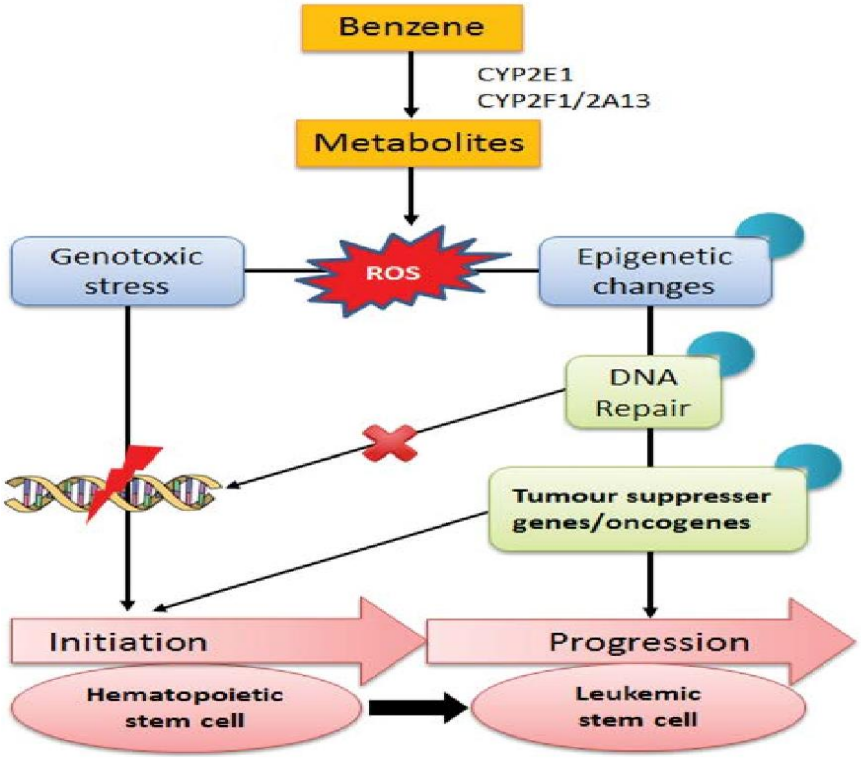

Figure 5 Mechanism of action of benzene in AML (Peng & Ng, 2016)

Chapter 2: Literature Review

2.1 Doxorubicin Chemotherapy

Doxorubicin is extracted from *Streptomyces peucetius* and is anthracycline antibiotic in nature. It is widely used as a traditional chemotherapeutic agent in various solid and hematological malignancies. Doxorubicin consists of two main components, sugar moiety and aglycones. The aglycone is made up of a tetracyclic ring with adjacent quinine-hydroquinone groups, a short side chain containing a methoxy substituent and a carbonyl group (Hilmer *et al*., 2004).

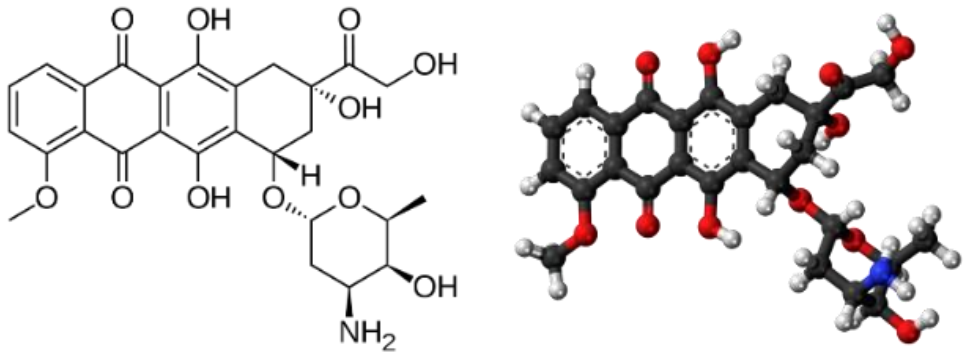

Figure 6 Molecular structure of doxorubicin (Ajaykumar, 2020)

2.1.1 Mode of Action

Doxorubicin produces wide range of cytotoxic effects by targeting various molecular signaling pathways by inducing apoptosis through intracellular targets. It has the ability to intercalate with DNA bases causing DNA double strand breaks thus inhibiting DNA and RNA synthesis. It also hinders the progression of the topoisomerase II, which is essential for replication, ultimately leading to apoptosis (Tacar *et al*., 2013).

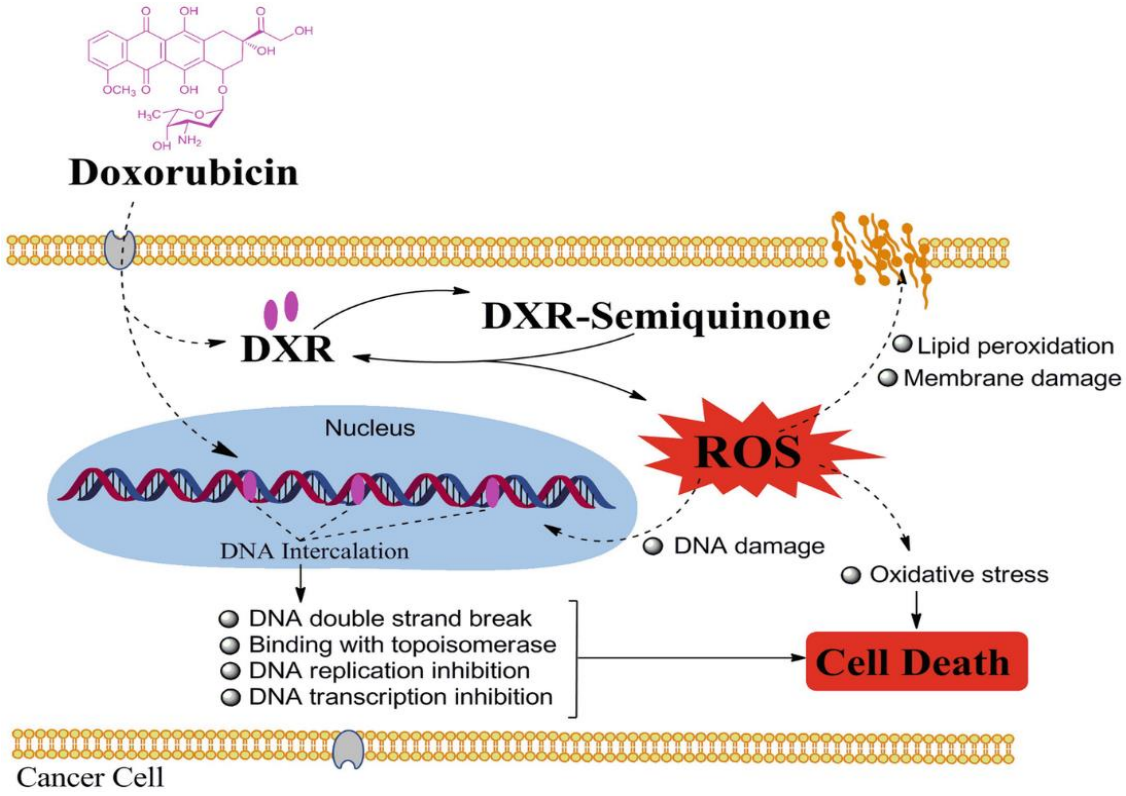

Figure 7 Mode of action of doxorubicin (Roychoudhury et al., 2020)

Doxorubicin possesses the ability to generate ROS that causes DNA, protein and cellular membrane damage. It stimulates the activation of AMPK pathway that triggers Bcl-2/Bax mediated apoptosis. Doxorubicin not only binds with DNA but is also capable of binding with mitochondrial DNA. These properties make it a potent anticancer drug. Doxorubicin therapy often exerts severe side effects, including damage to normal cells as well as renal, hematological and cardio-toxicity which limits its use and efficacy (Zanden *et al*., 2021).

2.2 Caffeine

Caffeine ($C_8H_{10}N_4O_2$) is a derivative of methylxanthine class (as shown in fig.)which acts as stimulant of human central nervous system. Being the most widely used and prescribed drug globally, it has attained legal status in many countries but still remains unregulated. It is bitter, methylxanthine alkaloid, white crystalline purine, and exhibit chemical resemblance to guanine and adenine

nitrogenous bases of ribonucleic acid (RNA) and deoxyribonucleic acid (DNA). It naturally exists in seeds, leaves and nuts as it helps to protect them from attack of predator insects. Coffee bean is the most well-known source of caffeine. Beverage products having caffeine are utilized to prevent lethargy and to improve performance.

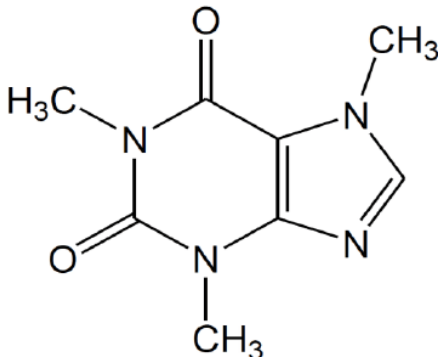

Figure 8 Structure of Caffeine (Kolachana et al., 1993)

2.2.1 Mode of Action

For decades, studies have been done to dissect the mechanisms of action of caffeine. Out of several known mechanisms, the most projecting one is show in figure 9.

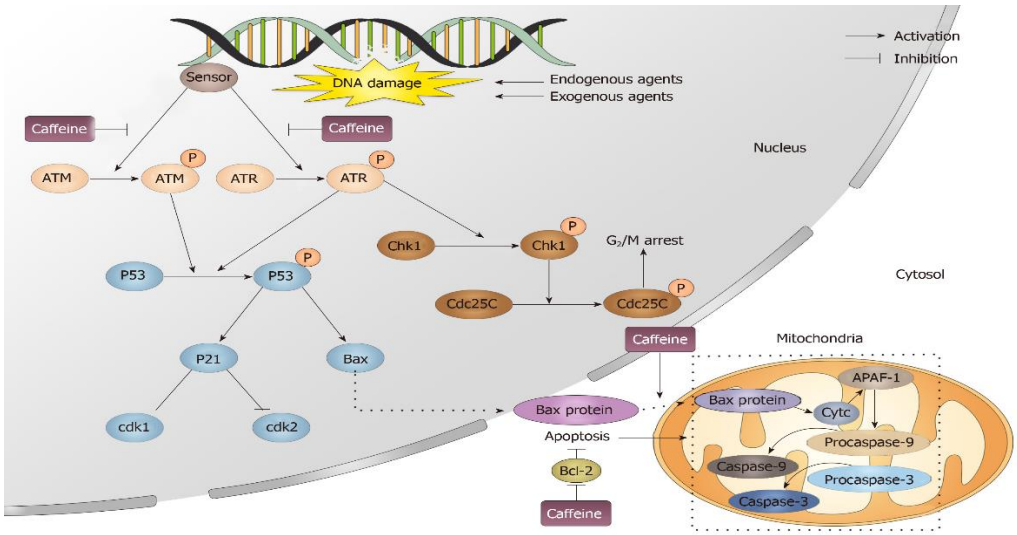

Figure 9 Mechanism of Caffeine Action

It is reported that the interaction of adenosine to its receptor is reversibly disrupted by caffeine which consequently prevents the onset of drowsiness and other affects induced by adenosine in human body. Likewise, certain other portions of our autonomic nervous system are also stimulated by caffeine. Caffeine causes extrusion by efflux pumps whose basal levels are regulated by transcription factor Pap1, to perform detoxification function (Hidalgo *et al.*, 2009). Caffeine does not activate Pap1 transcription factor rather it shuttles between cytoplasm and nucleus to regulate the expression of around fifty genes. Several toxic effects are induced by caffeine along with interference in cellular activities like in protein trafficking and general fitness impairment, cell wall damage, cell cycle arrest and DNA damage.

2.3 Use of Nanomedicine in Therapeutics

Novel Drug Delivery Systems (NDDS) offer numerous advantages compared to traditional medication methods. Traditional medication forms, like tablets and capsules, often fall short in delivering consistent and targeted effects over a treatment duration. These conventional methods may not ensure targeted delivery, might exhibit suboptimal pharmacokinetics, and can sometimes have unfavorable biopharmaceutical attributes. Such limitations can lead to issues like increased toxicity, side effects from frequent dosing, and, most critically, drug resistance.

To overcome these challenges, innovative solutions such as nanoparticles, liposomes, dendrimers, nanospheres, and carbon nanotubes have been introduced. These modern drug delivery mechanisms not only enhance therapeutic safety and effectiveness but also ensure precise drug delivery to the intended site. The recent advancements in carrier systems have shown potential in delivering multiple drugs simultaneously, even if these drugs vary in their therapeutic actions and physical-chemical properties. Such cutting-edge techniques prioritize drug delivery patterns, improved pharmacokinetics,

and enhanced drug bioavailability. Nanostructured systems are emerging as promising tools in pharmaceutical innovation, enhancing the stability of both water and lipid soluble drugs.

2.3.1 Drug Delivery System

There are following reasons to create drug delivery system:

- Distribution of drug can be controlled by incorporating it in carrier system.
- Molecular structure of the drug can be altered.
- Input of drug to bioenvironment can be controlled to confirm programmed and desirable biodistribution.

2.3.2 Nanomedicine Specificity/ Targeting

Target and carrier are two major components of drug targeting. Target is chronic or acute group of cells/organ which needs to be treated, while carriers are special molecules attached to drug which changes its structure at molecular level and transport drug to target specific sites. There are four types of drug targeting so far:

2.3.3 Passive Targeting

In case of malignancy, tumor micro-environment containing endothelial tissues along its surroundings becomes porous. These pores allow entry of drug coated nanoparticles by passive diffusion to enter the tumor tissue. Such mode of entry is termed as passive targeting. In this type of targeting, normal cells can be distinguished from cancerous cells i.e. direct access to cancerous cells and reduced toxicities to normal cells (Haley & Frenkel, 2008).

2.3.4 Active Targeting

Specific receptors are present on tumor sites which can be attached to specific ligands. Those ligands are attached to surface of drug loaded nanoparticles. Ligands of over-expressed receptors on tumor

sites and not expressed in normal cells are considered ideal ligands because they ensure drug delivery to tumor tissues only. This mode of targeting is called active targeting (Danhisher *et al.,* 2010).

2.3.5 Stimuli Responsive Drug Delivery

Nano-carriers are used to deliver drug to specific sites in response to some external stimulus. Drug is not released to pathological site until some stimulus is present. External stimuli could be heat, ultrasound and magnetic field. Such type of targeting is called stimuli responsive/ triggered drug delivery (Lammers *et al.,* 2012).

2.3.6 Targeted Drug Delivery

Delivery of drug to particular pathological site is challenging due to low efficiency, non-specific targeting, uncontrolled release and unequal distribution of drug to desired site. Controlled drug delivery system (DDS) could be the solution instead of traditional forms of drug *(Wilczewska et al.,* 2012). Drug delivery system can increase the efficiency, control specific targeting and provide higher concentration of drug to specific target sites (Allen, 2004).

Drug delivery system can be formed by keeping following points in mind:

- Stability and shelf life.
- Functionality and high encapsulation efficiency.
- Site specific transport of drug.
- Biodegradability.
- Biocompatibility.
- Drug uptake capacity.
- Zero premature release.

2.4 Liposomes

Liposomes are one of the most significant drug delivery systems developed within the field of nanomedicine. Liposomes, which are spherical structures formed by lipid bilayers, can contain both water-loving (hydrophilic) and fat-loving (hydrophobic) drugs, presenting a flexible system for directing medications to specific body sites (Holban & Grumezescu, 2016).

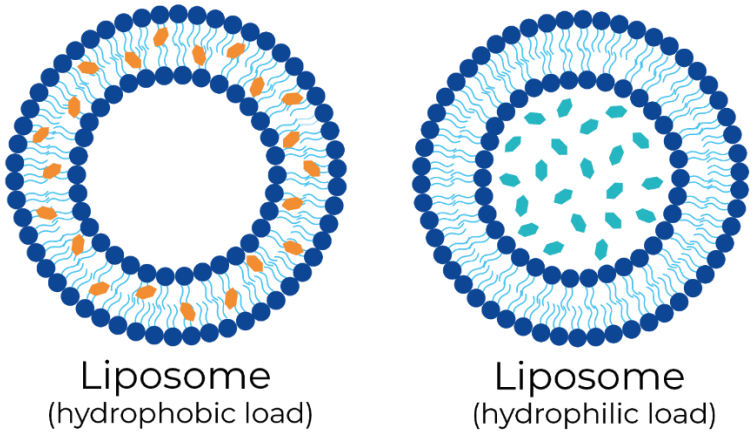

Figure 10 Hydrophobic and Hydrophilic Liposomes

2.4.1 Discovery and Evolution

Liposomes were first described by Alec D. Bangham in 1965, and since then, they have undergone extensive development. The evolution of liposome technology has been driven by the need to improve drug solubility, increase bioavailability, and reduce the side effects associated with conventional drug delivery methods.

2.4.2 Advancements in Clinical Applications

Over the decades, liposomes have transitioned from experimental systems to approved drug delivery vehicles. They have been successfully incorporated into several marketed pharmaceutical products, transforming the treatment landscape for various conditions, particularly cancer.

2.4.3 Structural Characteristics of Liposomes

A liposome's basic structural unit is the lipid bilayer, which closely mimics the architecture of biological membranes. This structural mimicry is fundamental to the liposome's ability to fuse with cellular membranes and facilitate drug delivery.

Liposomes are classified by size—ranging from small (less than 100 nm) to large (up to several micrometers)—and by the number of lipid bilayers, from single unilamellar vesicles to multilamellar concentric structures.

The surface of liposomes can be modified with various molecules to enhance their stability, prolong circulation time, and improve targeting. These modifications include the addition of polymers like polyethylene glycol (PEG), targeting ligands, and other functional groups (Powers & Nosoudi, 2019).

2.4.4 Encapsulation and Release

Liposomes can encapsulate drugs within their aqueous core or within the lipid bilayer, protecting them from degradation. The release of the encapsulated drug can occur passively, through diffusion or bilayer disruption, or actively, in response to environmental triggers like pH or temperature.

2.4.5 Cellular Interaction and Uptake

Once administered, liposomes interact with cells through various mechanisms, including adsorption, endocytosis, and membrane fusion. These interactions facilitate the delivery of the liposomal contents directly into the target cells.

2.4.6 Targeting and Accumulation

Liposomes can be designed to accumulate preferentially at specific sites within the body, such as tumor tissues, by exploiting pathophysiological conditions like the enhanced permeability and retention (EPR) effect.

2.5 Liposomal Components

2.5.1 Phospholipids

Phospholipids, the primary building blocks of liposomes, determine the physiochemical properties of the vesicle. The choice of phospholipid species, as well as the length and saturation of fatty acid chains, affects the fluidity, stability, and permeability of the liposome.

2.5.2 Cholesterol

Cholesterol is often incorporated into the liposome bilayer to modulate membrane fluidity and permeability. It provides structural integrity and can influence the release profile of the encapsulated drugs.

2.5.3 Surface Modifiers

Surface modifiers such as PEG, antibodies, or peptides can be added to liposomes to confer "stealth" properties, reduce immunogenicity, and enhance targeting to specific cells or tissues.

2.6 Liposome Synthesis and Production

2.6.1 Methods of Preparation

Liposomes can be prepared using various techniques, including thin-film hydration, sonication, extrusion, and microfluidics, each offering control over the size, homogeneity, and physical attributes of the liposomes.

2.6.2 Scale-Up and Manufacturing

Translating liposome production from the laboratory to industrial scale requires consideration of factors such as batch-to-batch consistency, sterility, and stability. Advanced manufacturing processes are being developed to meet the stringent requirements for clinical application.

2.7 Clinical Applications

Liposomal drug formulations are currently used in the treatment of cancer, fungal infections, and pain management, among others. They have significantly improved the therapeutic profiles of traditional drugs, such as doxorubicin in Doxil® and amphotericin B in Ambisome®.

Ongoing research is focused on developing next-generation liposomes with enhanced targeting capabilities, responsive release mechanisms, and multifunctional properties for combination therapy.

While liposomes have achieved notable success, challenges remain in optimizing their design, understanding their in vivo behavior, and overcoming biological barriers. Future directions include the development of personalized liposome-based therapies and the exploration of their potential in gene therapy and vaccine delivery (Akbarzadeh et al., 2013).

2.8 Therapeutic Index

Nano-formulation in medicine is spreading swiftly to increase drug uptake and delivery to specific sites. Nanoparticles are used in this case because they have the potential to reduce toxicities caused to healthy cells due to this increased therapeutic index. Therapeutic index is the comparative analysis of the efficacy of drug on pathological tissues to the cytotoxicity it causes to other normal tissues (De Jong & Borm, 2008).

2.9 Aims and Objectives

The aim of this research was to contribute in improved prognosis of Acute Myeloid Leukemia. The study had following objectives:

1. To develop a targeted Drug Delivery System (DDS) and find whether is it effective against acute myeloid leukemia or not.
2. To increase the half-life of caffeine in blood stream and examine its anti-cancer potential against acute myeloid leukemia.
3. To determine the changes in Blood Parameters and Cells Morphology after nanomedicine administration.
4. Analyzing the Hepatic and Renal Biomarkers.
5. To analyze Tissue Morphology and Organ Weights post therapy.

Chapter 3: Materials and Methodology

The lipid compounds DPPC (dipalmitoyl phosphatidylcholine), and DMPC (1,2-Dimyristoyl-sn-glycero-3-phosphocholine) along with Cholesterol, the drugs caffeine and doxorubicin, and Polyethylene glycol (PEG) of molecular weight 1000, were all procured from Sigma-Aldrich United States. Male Wister rats were purchased from the Animal House at the Atta-ur-Rahman School of Applied Biosciences (ASAB) of the National University of Sciences & Technology (NUST) in Islamabad.

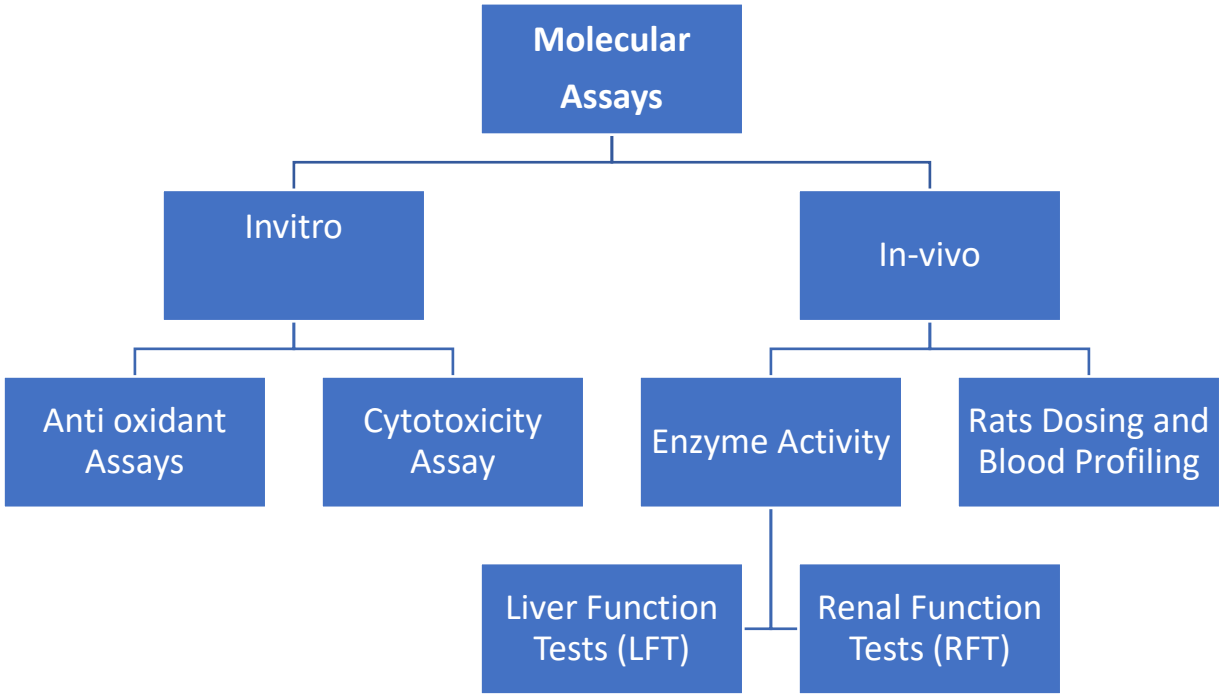

Figure 11 Study design to obtain desired goals

3.1 Synthesis of Caffeine-loaded and Doxorubicin-Loaded Nanoparticles

The synthesis involved using DMPC, DPPC, and Cholesterol in a molar ratio of 4:1:1. Initially, these lipids were dissolved in ethanol to make a 100μM solution. Separately, Caffeine and Doxorubicin were

each prepared in 200µM solutions using ethanol. From these solutions, 500µL was taken and combined with the lipid solution. This mixture was then sonicated for 40 minutes at 80MHz. Both the water and lipid phases were independently heated in water-bath until they attained 60°C. They were then combined and the resulting mixture was stirred for 10 minutes at 90 RPM. The combined mixture underwent another sonication, this time at 50MHz for 40 minutes. The excess ethanol was then evaporated using rotary evaporation at temperatures exceeding 50°C. The resulting blend of Caffeine and Doxorubicin-loaded and blank liposome nanoparticles was diluted to 50ml. At this stage, 0.25% of PEG (1000) was gradually added while continuously stirring. The mixture was then subjected to another round of rotary evaporation until only 10ml remained. Lastly, any drug that wasn't encapsulated was removed using a dialysis tube that had a diameter of 18/32 – 14.3mm and a pore size ranging from 12-14000 Daltons.

Table 2 Chemicals involved in Synthesis and loading of liposomal nanoparticles (LNPs)

No.	Chemical Name	Chemical Formula	Function
1.	DMPC	$C_{40}H_{80}NO_8P$	Bilayer Component
2.	DPPC	$C_{40}H_{80}NO_8P$	Bilayer Component
3.	Cholesterol	$C_{27}H_{46}O$	Membrane Fluidity
4.	Ethanol	C_2H_5OH	Solvent
5.	Polyethylene Glycol (PEG)	$(C_2H_4O)_nH_2O$	Polymer compound for coating of nanoparticles.

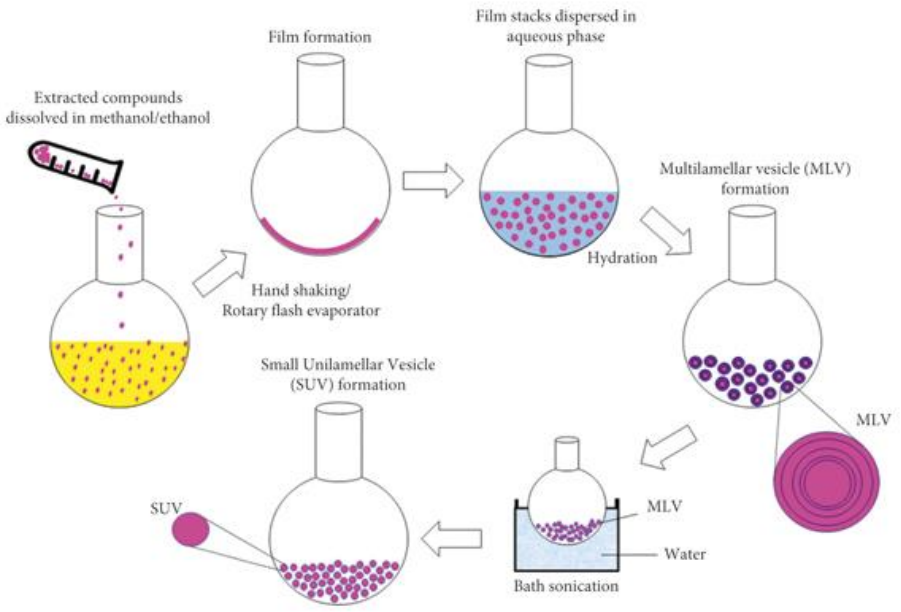

Figure 12 Steps involved in the synthesis of Liposomes

3.2 Characterization of nanoparticles:

The evaluation of morphology, particle size, drug encapsulation efficiency, zeta potential, release dynamics, and polydispersity index of Caffeine and Doxorubicin-loaded nanoparticles was achieved using various analytical techniques.

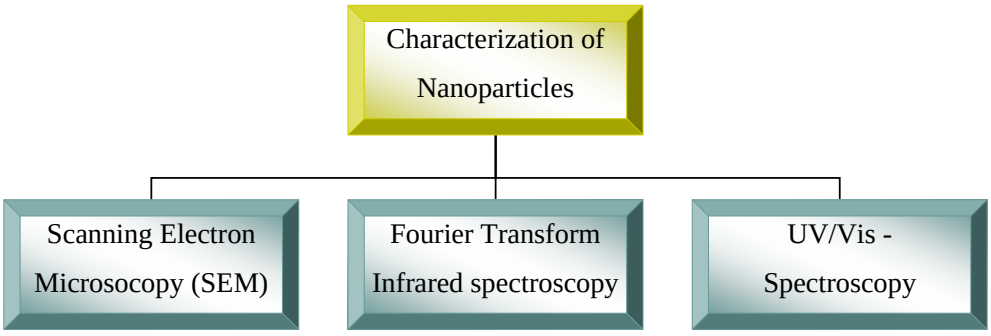

Figure 13 Techniques used for nanoparticles analysis

3.2.1 Scanning Electron Microscopy (SEM)

Scanning Electron Microscopy (SEM) was employed to examine the morphology of the liposomes. A small liposome sample was affixed to a glass coverslip, air-dried, and sputter-coated with a conductive layer. SEM imaging was conducted at XX kV, revealing liposome size, shape, and surface features. Image analysis software determined average size and distribution. SEM offered valuable insights into liposome morphology, aiding our understanding of their physical characteristics.

3.2.2 U.V-Vis Absorption Spectroscopy

Ultraviolet-visible (UV-Vis) spectroscopy is a widely utilized analytical technique in chemical and clinical research settings. This method quantifies the degree of light absorption by a sample when subjected to light irradiation, with the level of absorption deduced from the intensity of the transmitted light. In practice, the incident light beam is divided, with one portion traversing the sample-filled cuvette for analysis while the other is directed through a reference cuvette containing only solvent. Absorbance readings can be taken at specific wavelengths or across a spectrum, generating a profile of absorbance across various wavelengths. The peak absorbance, termed the lambda max, occurs at a distinct wavelength. This technique is instrumental in evaluating electronic transitions within molecules and adheres to the principles of the Beer-Lambert Law, which posits that absorbance (A) is the product of molar absorptivity (E), the concentration of the solute (c), and the path length (L) of the cuvette:

$$\mathbf{A=E\cdot C\cdot L}$$

Molar absorptivity, a comparative measure of how substances absorb light, is directly proportional to the molar concentration within the sample cuvette. This relationship allows for UV-Vis spectroscopy to serve as a reliable method for quantitative analysis.

The UV-Vis absorption spectra for blank nanoparticles as well as for caffeine and doxorubicin-loaded

nanoparticles were recorded using a Shimadzu UV-Vis 2800 BMS Scientific Technical Corporation (PVT) spectrophotometer. Measurements were measured over a wavelength 200-450 nm with resolution of 1 nm, employing deionized water as the reference medium. Spectra for the caffeine drug, PEG-coated caffeine nanoparticles, blank nanoparticles, free doxorubicin, and doxorubicin-loaded nanoparticles were all obtained for comparative analysis.

3.2.3 Fourier transform infrared spectroscopy (FTIR) analysis

Infrared (IR) spectroscopy is a methodical analytical approach primarily employed for identifying organic compounds and, to a lesser extent, inorganic materials. The principle underlying this technique involves the measurement of infrared radiation absorption by the sample as a function of wavelength.

The characteristic absorption peaks observed in the infrared region are indicative of the molecular constituents and the structural framework of the sample. Upon exposure to infrared light, molecules within the sample become vibrationally excited, transitioning to a higher energy state as they absorb the IR radiation. The energy differential between this excited state and the molecule's ground state dictates the specific wavelength of IR light absorbed by each type of molecule. Consequently, the unique absorption wavelengths serve as a molecular fingerprint, elucidating the sample's molecular structure.

Prior to FTIR analysis, samples were desiccated in air and then prepared using the KBr pellet method. The FTIR spectra were acquired using a Bruker FTIR Spectrophotometer ALPHA II, spanning a wavenumber range from 4000 to 350 cm^{-1} . Comprehensive FTIR spectral analysis was conducted for all the formulation components, including DMPC, Cholesterol, Caffeine, Doxorubicin, Blank liposomes (BNPs), Pegylated-Caffeine loaded liposomal nanoparticles and Pegylated- doxorubicin loaded liposomal nanoparticles.

3.2.4 Particle size and Area Distribution

Scanning electron microscopy (SEM) was deployed to determine the morphological size of the nanoparticles. The area distribution of the nanoparticles was quantified using ImageJ software. This involves selecting a field of view for analysis and applying the 'Analyze Particles' function to count and measure objects within binary or threshold images. The function initiates a scan across a designated area or image to detect the periphery of an object. The particle size data are presented within the range of 0 to 'Infinity,' with particles exhibiting circularity values outside the set parameters being excluded from the analysis. The process entailed examining an 8-bit binary image for the most accurately fitting ellipse corresponding to the profile of each particle observed.

For imaging purposes, a small aliquot of each nanoparticle sample type (BNPs, Caffeine, and Doxorubicin nanoparticles) was deposited onto a cover slip using a micropipette. Subsequently, gold sputtering was performed over the slide for 50 seconds at a current of mA to enhance conductivity and image quality. The images were captured using the VEGA3 LMU scanning electron microscope situated at the National University of Science and Technology, Islamabad. Furthermore, the size distribution and polydispersity of the nanoparticles were characterized using DLS with a Malvern Zeta Sizer Ver. 7.12 instrument.

3.2.5 Zeta Potential

The zeta potential signifies the electrical charge difference at the interface between a solid particle and the surrounding fluid. It is an indicator of the charge a particle carries when suspended in a liquid medium. Although zeta potential does not directly correspond to the actual surface potential within the double layer or the Stern potential, it is often the only accessible metric to characterize the double-layer properties in a colloidal system. Expressed in millivolts (mV), this parameter is also known as

the electrokinetic potential. Instruments that measure zeta potential can ascertain the surface charge and the zeta potential itself. The zeta potential provides insight into the stability, surface charge, and average size of nanoparticles. In colloidal science, zeta potential is the difference in electric potential across the ionic atmosphere surrounding a charged colloidal particle, essentially the potential at the boundary where the double layer's fluid phase flows past the stationary layer. Generally, the greater the zeta potential, the more stable the colloid, as higher charges prevent particle aggregation. A colloid will tend to coagulate when its zeta potential approaches zero. The surface charge and zeta potential of two types of liposomal nanoparticles (BNPs, Dox-NPs and Caffeine-NPs) were characterized using DLS with a Malvern Zeta Sizer Ver. 7.12 instrument.

3.2.6 Drug Encapsulation and Release Efficiency

Encapsulation efficiency refers to the proportion of the drug that is successfully confined within the vesicles of the liposomes. To ascertain this metric, a reliable linear standard curve was generated by measuring the absorbance of various drug concentrations at 280 nm using a UV spectrophotometer. This yielded an equation of the form Y=mx+c, which facilitates the determination of the encapsulated drug's concentration. The concentration of the drug that remained unencapsulated was deduced by applying the standard curve to readings obtained from the supernatants of centrifuged samples. These samples were subjected to centrifugation at 4500 rpm for a duration of 1 hour. The clear supernatant was then subjected to UV-visible spectroscopic analysis to quantify the unencapsulated drug fraction. This method follows the procedure outlined by Nii and Ishii (2005), with the encapsulation efficiency being computed using the established formula and the derived data points.

$$\textit{Encapsulation Efficiency} = \frac{\textit{Total drug} - \textit{Unentrapped drug} \times 100}{\textit{Total drug}}$$

3.2.7 Drug Release

The release kinetics of drugs from nanoparticulate carriers is pivotal for the efficacy of nanotherapeutics. The targeted and temporal control of drug release is a critical feature of nanoparticle formulation, aimed at achieving a controlled or sustained release profile. The drug release from PEGylated LNPs was monitored over a 48-hour period, with the inclusion of a precise volume of Phosphate Buffered Saline (PBS) to simulate physiological conditions.

For the release study, 3 mL aliquots from 25 mL solutions of blank nanoparticles (BNPs), PEG-coated Doxorubicin liposomes, and PEG-coated Caffeine nanoparticles were transferred into individual centrifuge tubes. These samples were then subjected to centrifugation at 4500 rpm for 10 minutes at ambient temperature. Concurrently, an equivalent volume of PBS was added to the remaining solutions of BNPs, PEG-coated Doxorubicin liposomes, and PEG-coated Caffeine nanoparticles. The supernatants were subsequently collected post-centrifugation for analysis via UV spectrophotometry.

This sampling and analysis procedure was repeated at specified time intervals, namely after 1, 2, 4, 6, 12, and 24 hours. At a wavelength of 280 nm, the absorbance was recorded and utilized to calculate the cumulative drug release. Throughout the study, a solution of empty nanoparticles served as the control to ensure accurate assessment of the drug release profiles.

3.3 In-Vitro Assays

A comprehensive set of assays was conducted to evaluate the biological efficacy of the unencapsulated drugs Caffeine and Doxorubicin, alongside blank nanoparticles, and PEG-coated liposomes loaded with Doxorubicin and Caffeine. Both in vivo and in vitro assays were carried out in strictly controlled environments, adhering to meticulously optimized protocols. A variety of instruments, materials, and molecular biology methodologies were employed to acquire the requisite data and outcomes.

Stock preparation for invitro assay

To evaluate the range of biological activities, serial dilutions of the drug solutions and nanoparticle dispersions were prepared. The nanoparticles were diluted to concentrations of 100%, 80%, and 60% of the original nanoparticle preparation using Phosphate Buffered Saline (PBS) as the diluent. For the drug solutions, 500 µL of a 4 mM drug stock solution was initially diluted in 10 mL of distilled water to create a primary stock solution. Subsequently, secondary dilutions of 80%, 60%, and 40% were made from this primary stock to facilitate the testing of various concentrations.

3.3.1 Brine Shrimps Assay (Cytotoxicity Assay)

The brine shrimp lethality assay is a straightforward and expedient method for assessing the cytotoxic potential of bioactive compounds. This assay gauges the ability of the substances under test to kill the simple organism Artemia salina, a species of brine shrimp. The assay was originally proposed by Michael et al. and has since been refined by various research groups. It is commonly employed to gauge the toxicity of substances such as heavy metals, pesticides, and pharmaceuticals, with a particular focus on natural plant extracts. The assay is considered a preliminary toxicity screening tool, providing an indication of potential hazards before conducting more complex studies involving mammalian animal models.

Table 3 Requirements for Brine Shrimp Assay

No.	Materials	Quantity	Company name
1.	Brine shrimp eggs	As required	Ocean star international, Inc
2.	Sea Salt	17g	
3.	Distilled water	500mL	-

For this purpose, brine shrimp eggs were allowed to incubate under room temperature and hatch under florescent light for 24 hours in sea salt solution. Sea salt solution was prepared by mixing 17g of sea salt in 500mL of distilled water (DW). To determine cytotoxicity at various concentrations, following dilutions were prepared in triplets:

These serial dilutions were kept in glass vials and dried overnight at room temperature. After this, 15 brine shrimps were counted under microscope and place in each vial for 24 hrs. The number of alive vs dead shrimps was then counted after 24 hours to calculate lethal concentration (LC 50 value) of dilutions.

Protocol

Artificial seawater was prepared to facilitate the hatching of brine shrimp eggs by mixing 17 grams of sea salt with 500 mL of distilled water. The pH of this synthetic seawater was maintained within a range of 8 to 8.5. The water was then oxygenated for two to three hours using a magnetic stirrer to ensure adequate aeration. A quantity of 10 mg of brine shrimp eggs was dispersed in the seawater and incubated at 37 °C for a period of 24 hours to allow for hatching.

Post-hatching, the phototactic instincts of the newly emerged nauplii (brine shrimp larvae) led them towards the illuminated portion of their environment. These nauplii were then collected using a 1 mL pipette for further testing.

In a 96-well plate, a microscope was used to ensure each well contained exactly 10 nauplii. To establish controls, triplicate wells were filled with ethanol as a positive control, indicative of 100% mortality, while saline filled triplicates served as the negative control, indicating no inherent toxicity. Various dilutions of the compounds under investigation—Caffeine, Doxorubicin (at 80%, 60%, and 40% concentrations)—along with their respective liposomal nanoparticle (LNP) formulations (at 100%, 80%, and 60% concentrations) were administered to the wells.

After a 24-hour exposure period, the survival rate was assessed by counting the number of surviving versus deceased nauplii in each well. Mortality rates were calculated using the formula:

$$Mortality(\%) = \frac{Mean\ dead\ shrimps\ in\ sample}{Total\ shrimps\ in\ sample}\ x100$$

The resulting mortality percentages were then graphically represented to visualize the cytotoxicity of the test substances.

3.3.2 Hemolytic Assay

The hemolysis assay is a critical in vitro test to determine the cytocompatibility of various substances by measuring the release of hemoglobin, which indicates the lysis of red blood cells (RBCs). In this assay, a fresh blood sample from a healthy male donor is collected in EDTA tubes to prevent coagulation. The sample is then diluted with PBS buffer and centrifuged to pellet the cells, which are subsequently washed and resuspended in PBS to their original volume.

Protocol

Test agents such as Caffeine, Doxorubicin, and their combination, along with their liposomal nanoparticle (LNP) formulations at various dilutions (100%, 80%, 60%, 40%), are prepared for the assay. A mixture of 100µl of RBC suspension and 100µl of each test solution is incubated at 37°C for 4 hours. PBS serves as the negative control, indicating no hemolysis, while Triton-X100 is used as the positive control, indicating complete lysis.

After incubation, the mixtures are centrifuged again, and the supernatant is transferred to a 96-well plate for absorbance reading at 550 nm using a microplate reader. The percentage of hemolysis is calculated by comparing the absorbance of the sample against a standard curve of lysed erythrocytes, with the formula taking into account the absorbance values of the positive and negative controls.

$$Percentage\ Hemolysis = \frac{Abs\ of\ test\ sample}{Abs\ of\ positive\ control}\ x\ 100$$

3.3.3 Total Antioxidant Capacity

Total Antioxidant Capacity (TAC) serves as a measure to evaluate the ability of a test solution to scavenge free radicals, thereby providing an overall assessment of the antioxidant potential present within biological samples. This assay is favored for several reasons, including its straightforward procedure, cost-effectiveness, rapid results, and the flexibility to be performed in a manual, semi-automatic, or fully automated manner. The assay utilizes the reduction of phosphate-molybdenum (VI) to phosphate-molybdenum (V) as its underlying principle.

Protocol

Initially, the required chemicals are accurately weighed. Specifically, 1.679 grams of NaH2PO4 and 0.247 grams of (NH4)2MoO4 are combined and dissolved in 50 mL of distilled water. To this solution, 1.63 mL of H2SO4 is added, resulting in the formation of the TAC reagent.

In the context of the antioxidant assay, distilled water is used as a negative control, indicating no antioxidant activity, while ascorbic acid, at a concentration of 1 mg/mL, serves as a positive control, providing a benchmark for antioxidant capacity.

A 96-well plate is prepared by adding 20 µL of each dilution of the test substances—Caffeine, Doxorubicin, and their liposomal nanoparticle formulations (LNPs) at concentrations of 100%, 80%, and 60%—in triplicate. To each well, 180 µL of the TAC reagent is introduced. Controls are set up with ascorbic acid and water in separate wells.

The plate is then incubated at 95 °C for 90 minutes, after which it is allowed to cool to room temperature. The absorbance of each well is measured at a wavelength of 695 nm. The TAC value is determined from the absorbance data using a formula that correlates absorbance to antioxidant activity. This calculated value provides an indication of each sample's antioxidant capacity, thus contributing to the understanding of its potential protective effects against oxidative stress.

$$Ascorbic\ Acid\ Equivalence = \frac{Absorbance\ of\ sample}{2.651}\ x\ 100$$

3.3.4 DPPH (1,1-diphenyl-2-picrylhydrazyl) Free Radical Scavenging Activity

The DPPH (2,2-diphenyl-1-picrylhydrazyl) assay is a widely used method to evaluate the free radical scavenging ability of various substances, due to the visually striking change from violet to colorless as the radical is reduced. This assay is based on the ability of antioxidants to transfer electrons to the DPPH radical, neutralizing its color and thus indicating the presence and potency of antioxidant activity.

Protocol

The DPPH assay is initiated by dissolving 3.9 mg of solid DPPH in 100 mL of methanol, which results in a 0.1 mM DPPH stock solution. This solution is further diluted with methanol to attain an optical density of 0.96 (±0.03) at 517 nm, which is necessary for the assay.

Distilled water is used as a negative control to provide a baseline, indicating no radical scavenging activity. In contrast, a solution of ascorbic acid at 3 mg/mL concentration serves as the positive control, representing a high level of antioxidant activity.

For the assay, 190 µL of the 0.1 mM DPPH solution is added to 10 µL of each dilution of the test substances (Caffeine, Doxorubicin, and their corresponding LNPs) prepared at concentrations of 80%, 60%, and 40%. The samples, along with controls, are placed on a 96-well plate.

The reaction mixtures are incubated in the dark at 37°C for 30 minutes to allow the reaction to proceed. Following incubation, the absorbance of each well is measured at 517 nm using the Thermo Scientific Multiskan Sky microplate reader. The half-maximal inhibitory concentration (IC50), is the sample required to scavenge 50% DPPH free radicals, and is plotted using Graph Pad Prism IC50 checker software version 5.

The free radical scavenging potential of each sample is calculated using a formula that relates the decrease in absorbance at 517 nm to the scavenging activity. This percentage indicates how effectively the sample can donate an electron to neutralize the DPPH radical, thus providing a quantitative measure of its antioxidant capacity.

$$Percentage\ Scavenging = \frac{Absorbance\ of\ control - Absorbance\ of\ test\ sample}{Absorbance\ of\ Control}\ x100$$

3.3.5 Total Reduction Power

The reducing power assay is a method used to evaluate the electron-donating capacity of antioxidants, which is indicative of their ability to exert antioxidant effects. The assay is based on the reduction of potassium ferricyanide (Fe^{3+}) to potassium ferrocyanide (Fe^{2+}), followed by the reaction of the ferrocyanide with ferric chloride to produce a colored complex.

Protocol

To prepare for the assay, reagents are constituted as follows: a 1% potassium ferricyanide solution is made by dissolving 1 gram of $K_3Fe(CN)_6$ in distilled water. A 10% trichloroacetic acid solution is obtained by dissolving 10 grams of trichloroacetic acid in 100 milliliters of distilled water. A 0.1% ferric chloride solution is also prepared by dissolving 0.1 grams of $FeCl_3$ in 100 milliliters of distilled water. Additionally, a 0.2M phosphate buffer is adjusted to a pH of 6.8 for use in the assay.

In the execution phase of the assay, each test sample is mixed with phosphate buffer and potassium ferricyanide and then incubated at 50°C for 20 minutes. Post-incubation, trichloroacetic acid is added, and the mixture is centrifuged to separate the layers. The upper layer of the mixture is then mixed with ferric chloride to complete the reaction.

For controls, ascorbic acid is used as the positive control due to its known reducing power, while distilled water serves as the negative control. The color change is indicative of reducing power and is measured spectrophotometrically at 700 nm using a microplate reader.

The absorbance values obtained are then used to calculate the reducing power of the test samples, expressed in terms of ascorbic acid equivalency. This reflects the antioxidant capacity of the samples, providing insight into their potential therapeutic efficacy as antioxidant agents.

$$Ascorbic\ Acid\ Equivalence = \frac{Absorbance\ of\ sample}{2.705}\ x100$$

3.4 Experimental Strategy

Male Wistar rats, each weighing between 100 and 150 grams and approximately 7 weeks of age, were procured from the ASAB animal house. Upon acquisition, the animals were assorted into various groups and underwent a seven-day acclimatization period where they had unrestricted access to both food and water. They were accommodated in standard laboratory cages, which were bedded with fresh sawdust and replenished every 48 hours to ensure cleanliness and comfort. The ambient conditions were carefully regulated, with temperatures maintained at a steady 27°C, with an allowable variation of ±2°C, and relative humidity controlled at 60% ± 5%. For each experimental leukemia model, the rats were allocated into seven distinct groups, each consisting of five subjects, in addition to one control group with normal conditions. The body weights of the rats were meticulously recorded on a weekly basis throughout the experimental and treatment phases. All procedures involving the handling and care of the rats adhered strictly to the 1978 FDA (Food and Drug Administration) guidelines for good laboratory practice.

Table 4 Dosing and mode of administration of drugs among different groups

No.	Groups	No. of Rats	Dosage Regime	Mode of Administration
1.	Control	5	Saline / Injection water	Intravenous
2.	Benzene	5	(100ul/ml) for 4 weeks alternatively.	Intravenous
3.	Caffeine	5	5mg/kg for 4 weeks alternatively.	Intravenous
4.	Doxorubicin	5	5mg/kg for 4 weeks alternatively.	Intravenous
5.	Blank Liposomes	5	(100ul/ml) for 4 weeks alternatively.	Intravenous
6.	Doxorubicin Liposomes	5	100ul from 4mM stocks prepared for 4 weeks alternatively.	Intravenous
7.	Caffeine Liposomes	5	100ul from 4mM stocks prepared for 4 weeks alternatively.	Intravenous

3.4.1 Administration of Benzene

Benzene injections were prepared by mixing 0.6ml benzene in 1.2ml Iso-propanol and 0.6ml injection water, keeping the aspect ratio as (1: 2: 1). Out of this mixture, 0.1ml of benzene was injected to each rat in seven groups labeled as Group 2, Group 3, Group 4, Group 5, Group 6, and Group 7. These injections were given intravenously for 4 weeks alternatively under standard and optimized conditions. Group 1 was considered as negative control, while rest of all were used for further dosage treatments after leukemia induction.

3.4.2 Administration of Caffeine

Caffeine powder was purchased from Sigma Aldrich (CAS No. 58-08-2) in its pure form. It was administered (5mg/kg for 4 weeks alternatively) to Group 3 after treatment with benzene injections.

3.4.3 Administration of Doxorubicin

Doxorubicin (10 mg with 5mL of injection water), a chemotherapeutic drug was purchased from Shaheen Pharmacy Rawalpindi. Stock solution of 3.75 mg /1.8 mL was prepared per day. It was administered (5mg/kg for 4 weeks alternatively) to Group 4 after treatment with benzene injections.

3.4.4 Administration of Nanomedicine

Blank liposomes, Doxorubicin liposomes and Caffeine liposomes were administered to Group5, Group 6 and Group 7 respectively. Each rat was injected with 100ul from 4mM stocks prepared for 4 weeks alternatively. The dosing of each group and mode of administration is given in table 2.4.

3.5 Animal Dissections

After completing all doses, all rats were dissected according to the rules of Institutional Animal Care and Use Committee (IACUC). It was done by laying rats on a dissecting board and surgical tools were used to cut the abdominal cavity. Body cavities of rats was exposed to obtain different organs *i.e.* heart, liver, blood and kidney.

3.5.1 Blood Collection and Storage

Heparinized syringes were used to take blood directly from heart and collected into the commercially available Ethylene Diamine Tetra Acetate (EDTA) tubes (purple color vacutainer) and serum tubes (yellow color vacutainer) instantly. EDTA tubes were stored at -4C while Serum tubes were centrifuged at 3000rpm for 15 min to separate serum and stored at -40 C to prevent hemolysis.

3.5.2 Organs Collection

All vital organs like heart, liver, and kidney were collected and preserved stepwise for further evaluation and expression analysis. Liver, found under diaphragm and is attached to many muscles, was removed with the help of scalpel and scissor. Heart being the main part of circulatory system is located in thoracic region and was removed likewise. Kidneys are bean shaped, primary organ of excretory system and located in the upper abdominal region. Kidneys were removed with the help of scalpel and shifted to normal saline and then to distilled water. All the organs were weighed by digital weighing balance and data was recorded for measuring Relative Organ Weights (ROWs).

3.5.3 Blood Profiling

For morphological analysis, blood smears were prepared upon glass slides using fresh blood after dissection. Smear was produced by sliding cover slip upon blood dot at 45° angle, first sliding backward little bit and then forward till the end of slide. These smears were then air dried and dipped in chilled absolute methanol for 10 minutes for fixation. After another round of air drying, GIEMSA staining was performed by pouring Giemsa dye dropwise upon smear for 10 minutes. The stained slides were washed with tap water and then air dried. These were observed under the light microscope at 100X lens to study the morphology of cells.

3.5.4 Blood Complete Picture:

To obtain total blood cell count, Blood CP was calculated upon an automated instrument that measures various parameters of blood. For this purpose, 100 ul blood was stored in EDTA tubes and transferred to Islamabad Diagnostic Centre for Blood CP. The complete picture included HGA, PLT, RBC, WBC and other cell levels in blood.

3.5.5 Enzymes Activity (Hepatic and Renal)

For evaluation of enzymes activity, Micro Lab 300 autoanalyzer (Merk) was used to perform biochemical assays. The parameters analyzed were ALP, ALP, AST and Renal Function Test (RFT) using biochemical analysis kits (AMP diagnostic kits).

3.5.6 Alkaline Phosphatase (ALP)

To estimate the quantity of alkaline phosphatase, standard protocols were followed provided by (AMP diagnostic kits). About 1mL of Reagent A was added in an Eppendorf tube following the addition of 20µL of serum. Solution was incubated for 1 minute at 37° C, then 250µL Reagent B was added. Micro Lab 300 autoanalyzer (Merk) was used for taking absorbance at 420nm for 1 minute. At least 3 readings were taken. Reagents mixture without sample was taken as blank.

A/min x 2757= ALP activity U/L at 37^0C

3.5.7 Alanine Aminotransferase (ALT)

ALT assay was performed by using LTA diagnostic kit. We used 1000µl of Reagent 1 (Tris buffer 100mM (PH 7.15), preservatives and stabilizers) and 250µl Reagent 2 (L-alanine 500mM, alpha-keto glutarate 12mM, NADH 0.18mM, LDH ≥ 1700 U/l) in an Eppendorf. Serum that was separated from the blood was used as sample. In Reagent 1, 125µl of sample was mixed by vertexing and left for 5 mins at room temperature. After adding Reagent 2, the mixture was introduced to autoanalyzer by its sipper and initial absorbance reading was recorded. Three readings were taken after every 1 minute to determine difference between absorbance values

A/min x 1746= ALT/GPT activity U/L at 37^0C

3.6 Statistical analysis

In vivo experiments were conducted to assess the impact of various therapeutic interventions on rat subjects. Data were presented as the mean ± standard deviation (SD), with statistical analyses performed using GraphPad Prism software. Significance was determined where a p-value was less than 0.05, indicating statistical relevance in each scenario. Comparative analysis among different groups was executed via one-way analysis of variance (ANOVA), with further differentiation among groups achieved through Tukey's post-hoc test.

Chapter 4: Results

4.1 Physical characterization of Caffeine and Doxorubicin NP's

Nanoparticles of Doxorubicin and Caffeine were synthesized using the thin film hydration technique, creating a bilayer vesicle comprised of DPPC, a phospholipid characterized by two C16 palmitic acid groups and often found in conjunction with lecithin, along with DMPC, which features myristoyl chains at the first and second positions on the glycerol portion. Following their assembly, these vesicles were enveloped with PEG, leading to the emergence of broadened peaks in their spectral profiles

4.1.1 UV-Visible Spectroscopy

The UV-Vis absorption spectra revealed characteristic peaks for cholesterol at 207 nm and PEG-1000 at 250 nm. The phospholipids, DMPC and DPPC, exhibited absorption maxima at 230 nm and 220 nm, respectively. Doxorubicin (DOX) demonstrated distinct peaks at 235 nm and 479 nm, while caffeine displayed its peak at 270 nm. The absence of peaks in the spectrum of the blank nanoparticles, which showed an absorbance at 230 nm, coupled with the observed shift in the absorbance peaks for DOX and caffeine in the nanoparticle formulations, suggests successful incorporation of cholesterol and PEG-1000 and the successful encapsulation of the drugs within the nanoparticles.

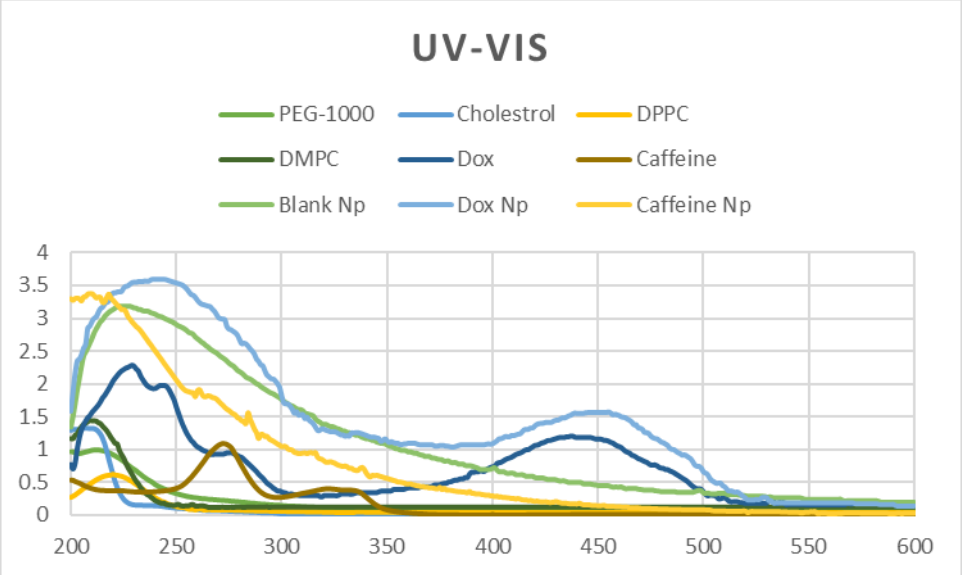

Figure 14 UV-Vis Spectrum absorption Spectroscopy of all drugs and constituent of nanoparticles

4.1.2 Zeta Potential

The average Zeta potential of Blank-Np, DOX-Np and Caffeine-NP was found to be -2.6, -7.26, and -5.6 mV respectively.

Table 5 Zeta Potential Values of Nanoparticles

Compound	Zeta Potential (mv)
Blank Nanoparticles	-2.6
Dox Nanoparticles	-7.26
Caffeine Nanoparticles	-5.6

4.1.3 Fourier Transform Infrared Spectroscopy (FTIR) Analysis

The FTIR spectrum of Blank NPs indicated peaks at 2919/cm (C-H stretch), 1632/cm (R-NH2, Amines), 1115/cm (C-O stretch), 720/cm (RCH2CH3), 1215/cm (P-0 stretch). The Doxorubicin

indicated peaks at 1372/cm (-C(CH3)2- stretch), 1304/cm (P-0 stretch), 2896/cm (CH3 stretch), 2896/cm (-CH3/-CH2 stretch), 1054/cm (P-O-C stretch). Caffeine NPs indicated peaks or bands at 2850/cm (C-H stretch), 3417/cm (O-H stretch), 1375/cm (C-O-H stretch), 873/cm (Tri-substituted Aromatics). By integrating drug and PEG 1000, the structural changes in lipid biomolecules were demonstrated by changes in infrared bands.

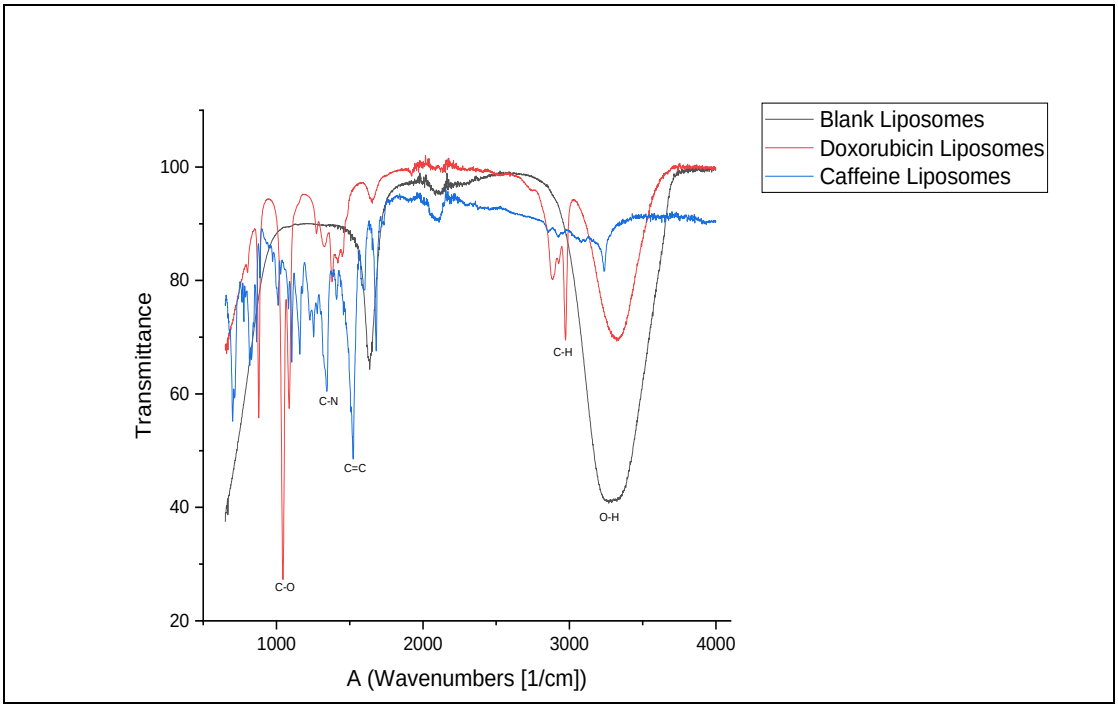

Figure 15 FTIR of BNPs, Dox-NPs, Caffeine-NPs

4.1.4 Particle Size and Area Distribution

The size of BLank-Nps, DOX-Nps and Caffeine-Nps was determined by the Scanning Electron Microscopy (SEM) and by using image j software the area distribution of the Np was measured. Scanning images showed the spherrical nanoparticles with the mean size of 35, 87, 74 nm for BLank-Nps, DOX-Nps and Caffeine-Nps respectively.

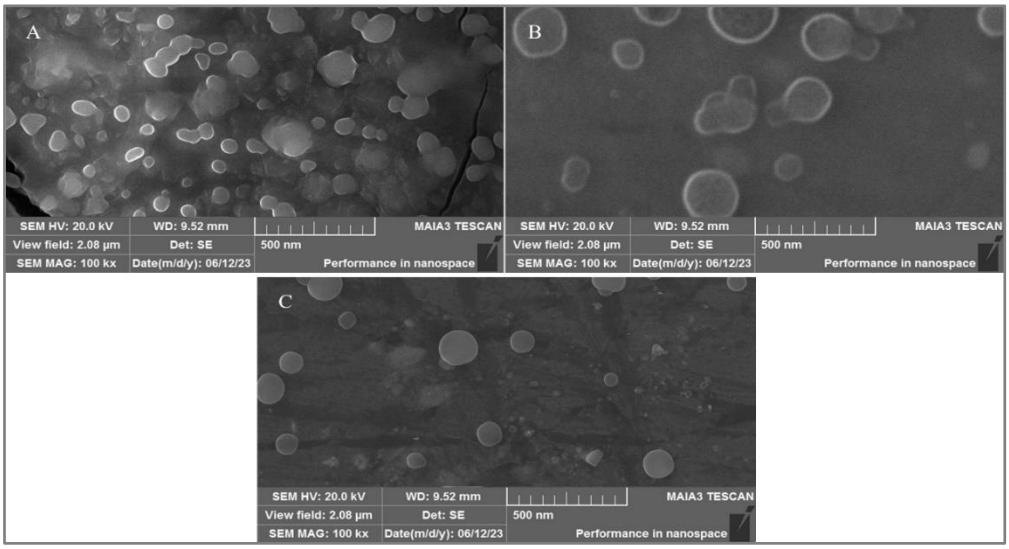

Figure 16 SEM of a)BNPs, b)Dox-NPs and c)Caffeine-NPs

4.1.5 Drug Encapsulation Efficiency

The encapsulation efficiency of DOX-Nps and Caffeine-Nps was found to be 78.87 and 74.62 % respectively explaining the entrapment of drug in nanoparticles respectively.

4.1.6 Drug Release Kinetics

The release of drug from Np were noted up to 16 hours suggesting the sustain released of drug with time. This long stay of drug helps in achieving high bioavailability and eventually leads to high efficacy in treating the diseases.

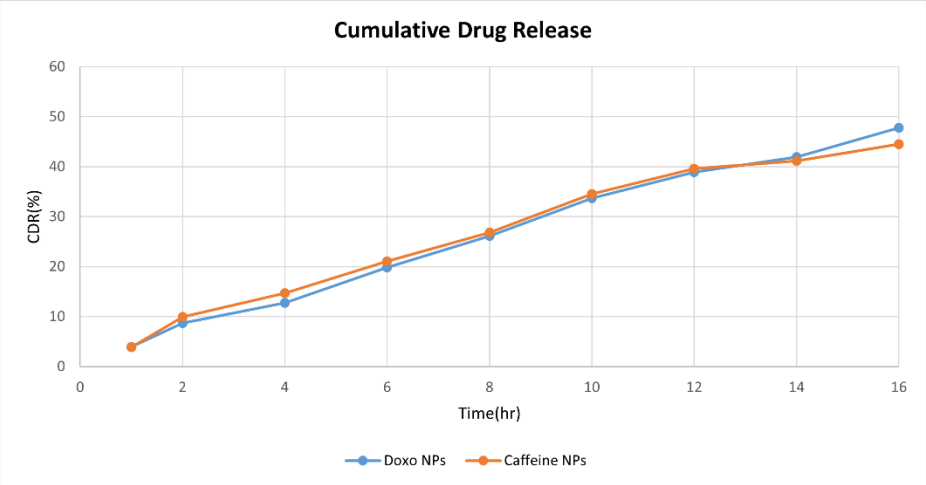

Figure 17 Drug Release Graph of Dox-NPs and Caffeine-NPs

4.2 In-Vitro Assay

4.2.1 Brine shrimp Assay

The percentage mortality of DOX-Nps and Caffeine-Nps at different concentrations were significant as compared to DOX, and Caffeine respectively, as shown in figure. The LC50 calculated for DOX, Caffeine, DOX-Np, and Caffeine-Np were 2213.3µg/ml, 1608.3µg/ml, 2856.0µg/ml, and 2094.7 µg/ml respectively, showed that drugs their nanoparticles were non-toxic according to criteria (Zheng & Bossier, 2023).

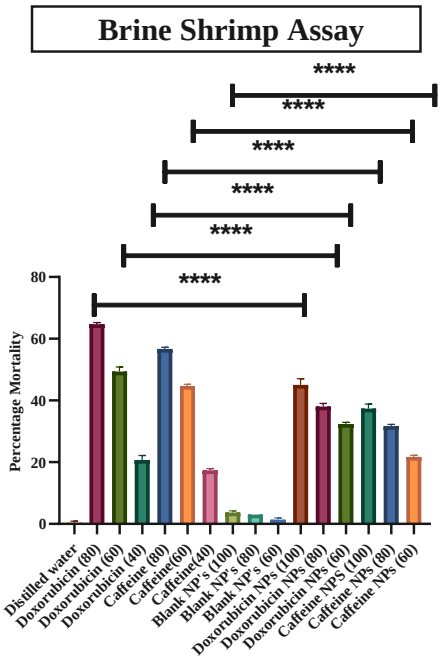

Figure 18 Comparison of %age mortality of brines shrimp

4.2.2 Hemolytic Assay

The percentage hemolysis of DOX-Np and Caffeine-Np at different concentrations were significant as compared to free DOX and Caffeine respectively, as shown in figure. The LC50 calculated for DOX, Caffeine, DOX-Np, and Caffeine-Np were 5783.8µg/ml, 4973.6µg/ml, 8311.7µg/ml, 8423.5µg/ml, 7888.9µg/ml and 7356.0µg/ml respectively, showed that drugs their nanoparticles were non-toxic according to criteria (Zheng & Bossier, 2023). According to ASTM F 756-00 standards (Dobrovolskaia et al., 2008) the designed nanoparticles were hence suitable for IV route and are biocompatible as they are less hemolytic than free drug.

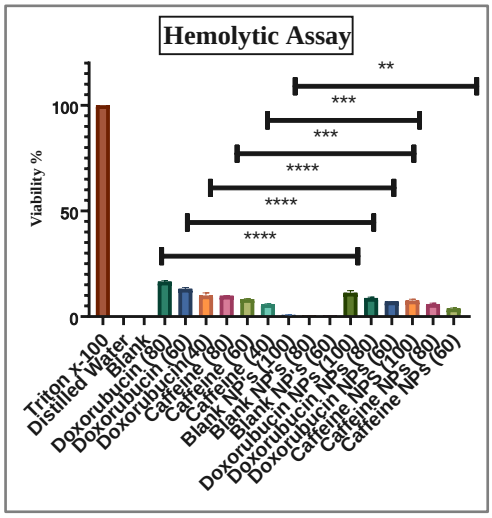

Figure 19 Comparison of %age viability of blood at different concentrations of Drugs and NPs

4.2.3 Total Antioxidant Capacity

The TAC of DOX-Np, and Caffeine-Np at different concentrations were significant (P<0.0001) in comparison to free drug as shown in figure which states that Np are biocompatible.

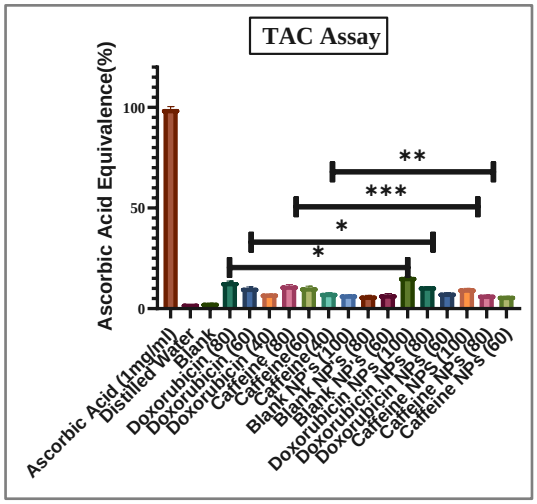

Figure 20 Comparison 0f Total Antioxidant Capacity values of free Drugs and NPs

4.2.4 DPPH Free Radical Scavenging Activity

The DPPH scavenging activity of DOX-Np, and Caffeine-Np at different concentrations were significant when compared to their free drugs respectively (P< 0.001).

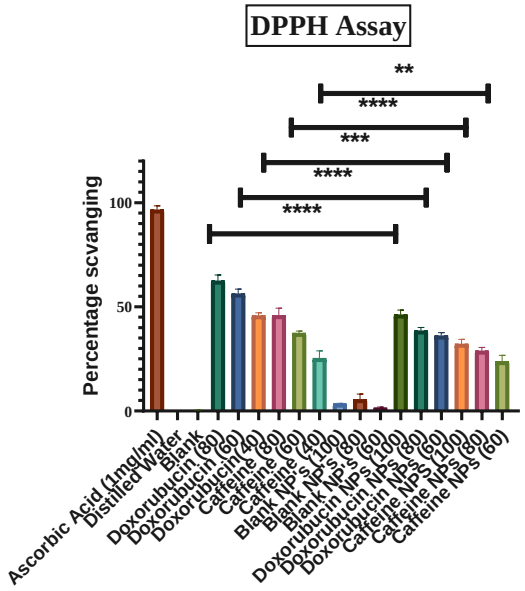

Figure 21 Comparison 0f DPPH scavenging percentages of free drugs and NPs

4.2.5 Total Reducing Power Assay

The TRP value of DOX-Np, and Caffeine-Np at different concentrations were more significant as compared to free drug (P < 0.0001) as shown in figure.

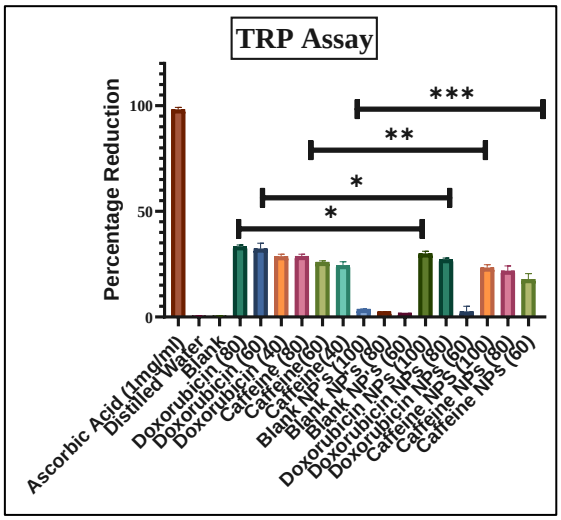

Figure 22 Comparison 0f Total Reduction Potential values of free Drugs and NPs

4.3 In vivo Assay

4.3.1 Body Weights

During the period of acclimatization body weight of all the rats increased. In the induction period the body weights of all the rats decreased over the time as compared to control group. The diseased group showed significant decline in body weights as compared to control group when t-test was applied ($P < 0.05$) as shown in fig . During the treatment period, significant increase in the body weights was observed in all treatment groups.

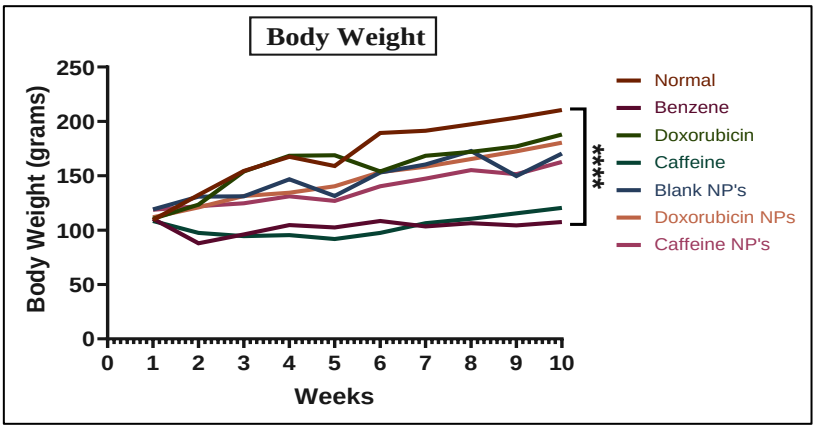

Figure 23 Average body weights of different experimental groups of rats

4.3.2 Organ weights

The organ weights were obtained at the time of dissections, which showed significant increase in organ weights in diseased group as compared to control. While one way ANOVA analysis displayed that treatment groups showed significant decrease in body weights of liver, heart and kidney as compared to disease group which is evident from graph as shown in figures.

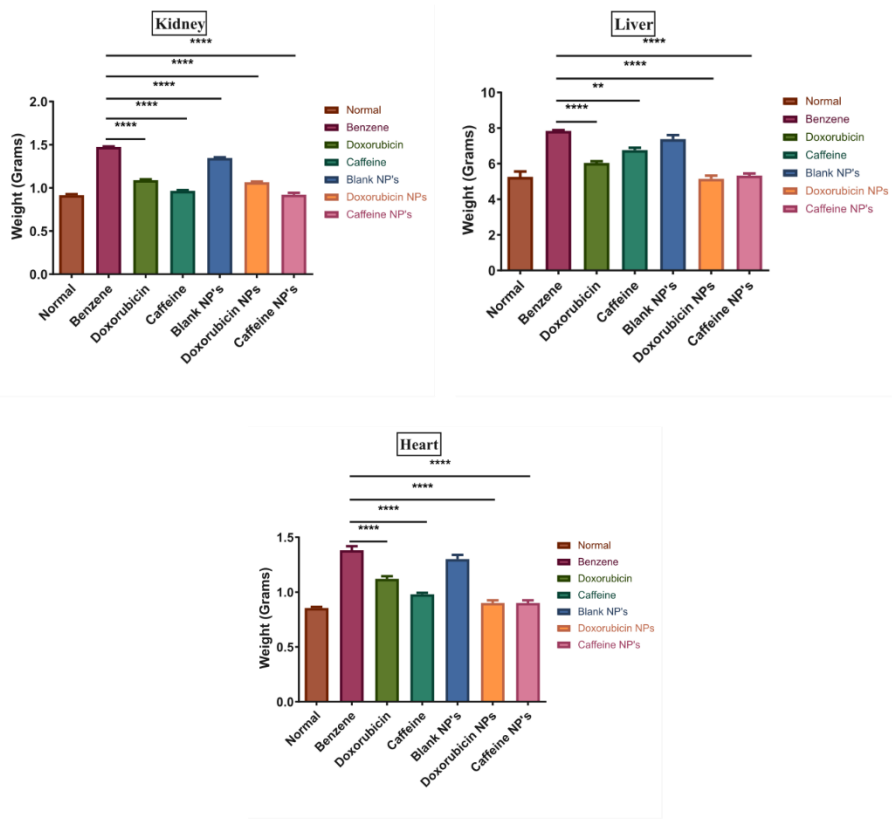

Figure 24 shows comparison of A) Kidney, B) Liver weight and C) Heart of different experimental groups

4.3.3 Serological Analysis

4.3.3.1 Liver Function Test

The results of liver function test including alkaline phosphatase (ALP), aspartate aminotransferase (AST), alanine transaminsae (ALT) showed significant decrease in the serum levels of ALP while significant increase in (AST) and (ALT) serum levels when benzene was given for induction. However, treatment groups showed significant decrease in serum level of AST, and ALT while a significant increase in ALP levels. The nanoparticles showed more significant results as compared to free drug as shown in figure.

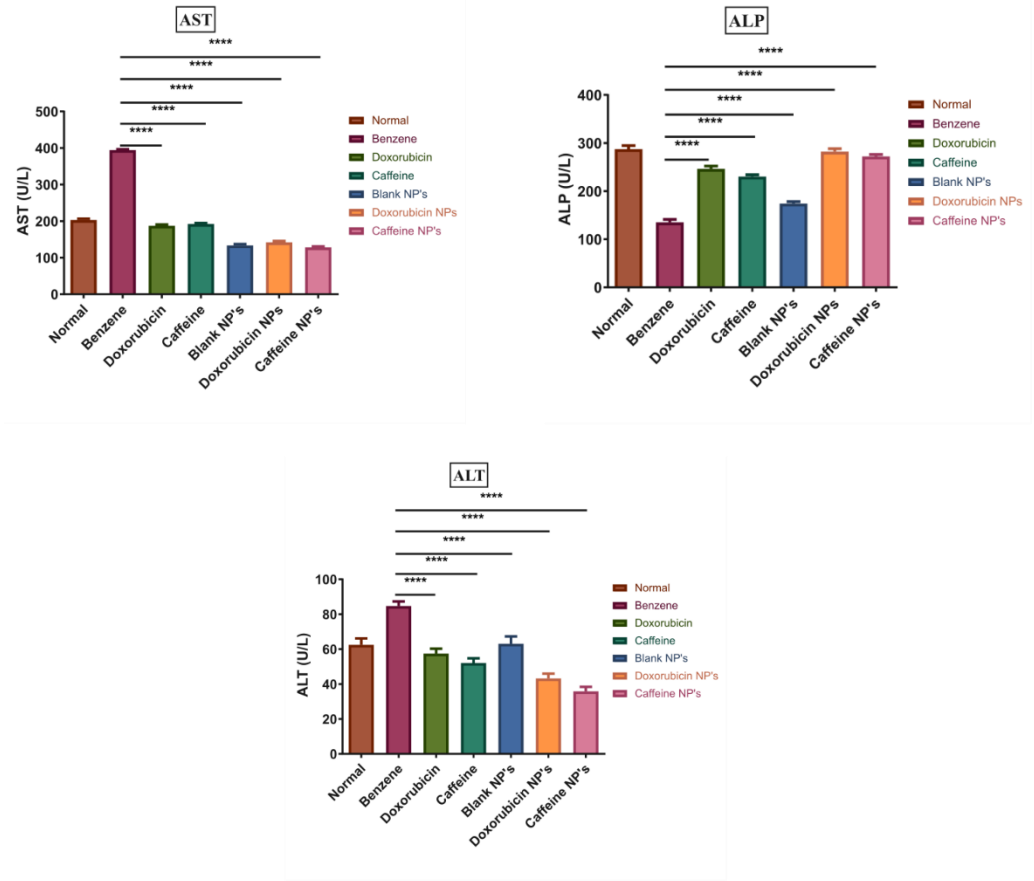

Figure 25 Comparison of Serum A) AST, B), ALP and C) ALT, in different experimental groups

4.3.3.2 Renal Function Test

The results of liver function test including creatinine, urea and uric acid showed significant increase in the serum levels of creatinine and uric acid while decrease in urea levels when benzene was given for induction. However, treatment groups showed significant decrease in serum level of creatinine and uric acid while significant increase in urea levels.. The nanoparticles showed more significant results as compared to free drugs as shown in figure.

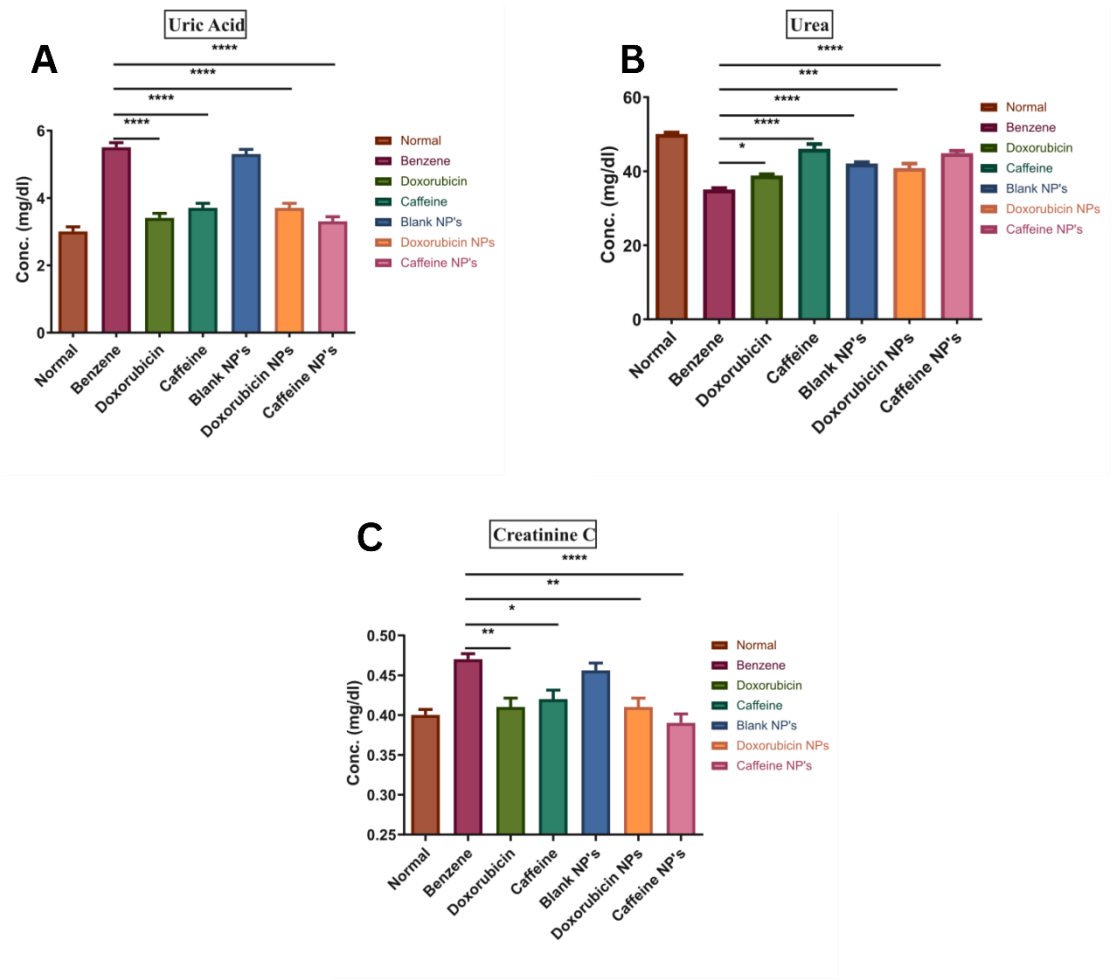

Figure 26 Comparison of Serum A) Uric Acid, B) Urea, and C) Creatinine C in different experimental groups

4.4 Complete Blood Count

To analyze the effects of different drugs upon blood cells count, complete blood count was obtained.

4.4.1 White Blood Cells

White blood cells were counted and visualized by complete blood picture. It was observed that the total WBC count significantly increased in group 2 (benzene treated rats) i.e. an indicator of leukemia.

This abnormal increase was restored in doxorubicin and caffeine treated groups. However, the nanoparticles showed more significant results as compared to free drugs as shown in figure.

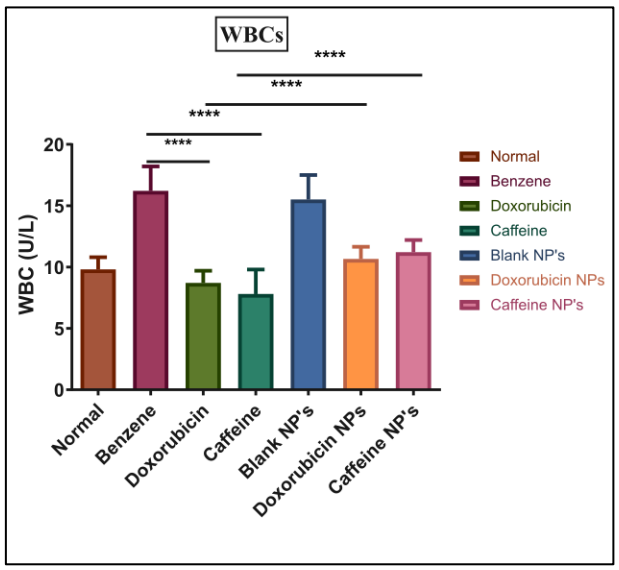

Figure 27 Comparison of Total WBC count in different experimental groups

4.4.2 Red Blood Cells

It was observed that the total Red Blood Cells count decreased signifcantly in Group 2. However treatment with doxorubicin andcaffeine nanoparticles exhibited a significant increase indicating restoration of normal RBC count. It was also learnt by applying ANOVA over these counts that the efficacy of Nanomedicine is significantly higher than the caffeine in restoring normal RBC count.

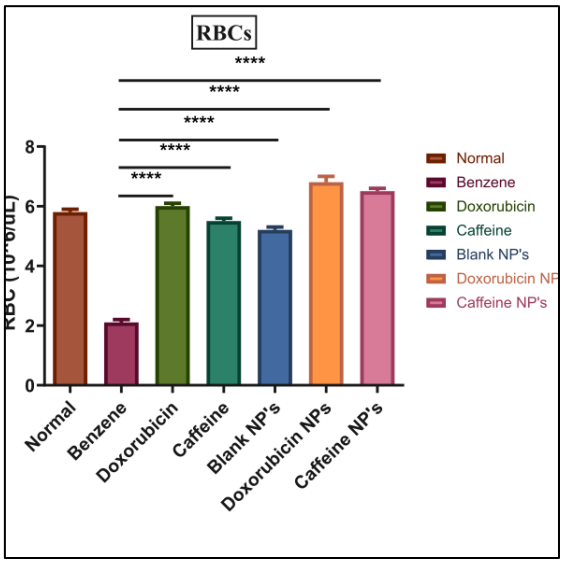

Figure 28 Comparison of Total RBC count in different experimental groups

4.4.3 Monocytes

It was observed by complete blood count that the number of monocytes increased significantly in benzene treated rats as compare to normal. However, Group 3 and 4 having Doxorubicin and Caffeine treated rats respectively, decreased monocytes count to normal. Such reduction was not observed in Group 5 i.e. Nanomedicine treated rats, instead showed more significant results as compared to free drugs as shown in figure.

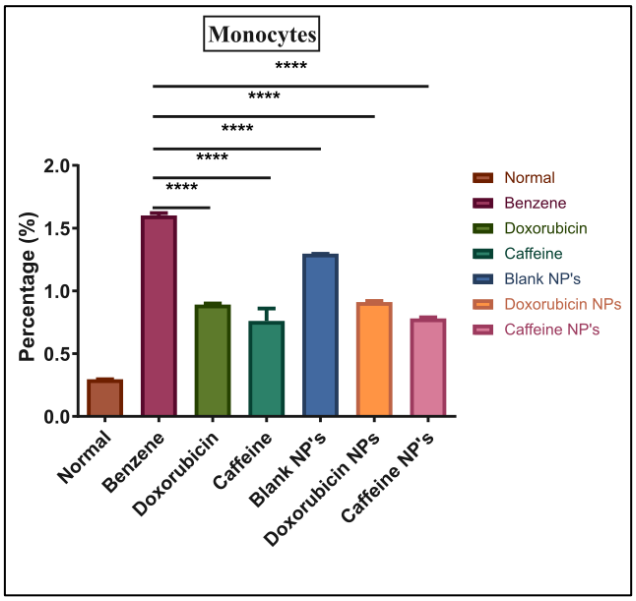

Figure 29 Comparison of Monocytes count in different experimental groups

4.4.4 Eosinophils

It was observed by complete blood count that the number of eosinophils increased significantly in benzene treated rats as compare to normal. However, Group 3 and 4 having Doxorubicin and Caffeine treated rats respectively, decreased eosinophils count to normal. Such reduction was not observed in Group 5 i.e. Nanomedicine treated rats (Group 6 and 7), instead showed more significant results as compared to free drugs as shown in figure.

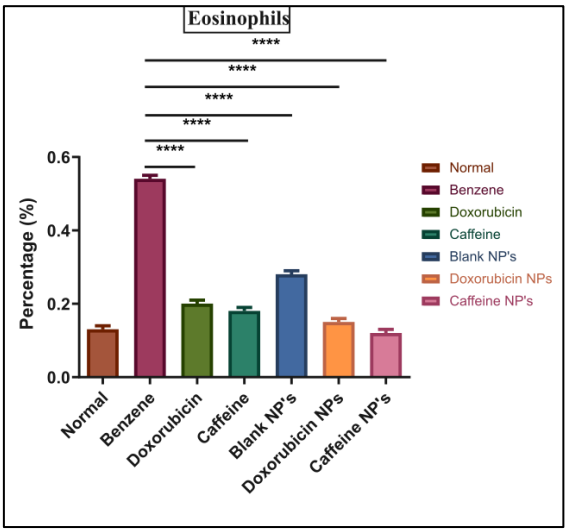

Figure 30 Comparison of Eosinophils count in different experimental groups

4.4.5 Neutrophils

After observing the number of neutrophils in experimental groups, it was noted that the neutrophils count increased slightly in leukemic rats. Treatment with doxorubicin and caffeine did not recover normal levels of neutrophils. Blank nanoparticles alone were also not that much effective however caffeine nanoparticles significantly reduced neutrophil levels in Group 7. The efficacy of caffeine increased by using it in the form of nanomedicine, as significant reduction in Neutrophils was observed in Group 7.

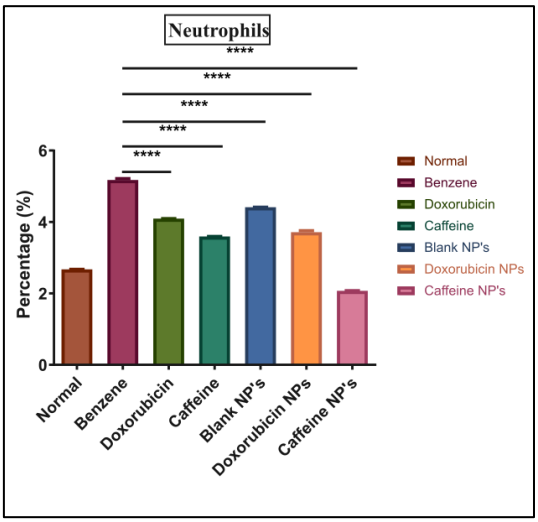

Figure 31 Comparison of Neutrophils count in different experimental groups

4.4.6 Lymphocytes

It was observed that the Absolute Lymphocytes Count (ALC) increased in beneze treated rats. Doxorubicin also showed same behaviour but caffeine being a potent anticancer therapeutic

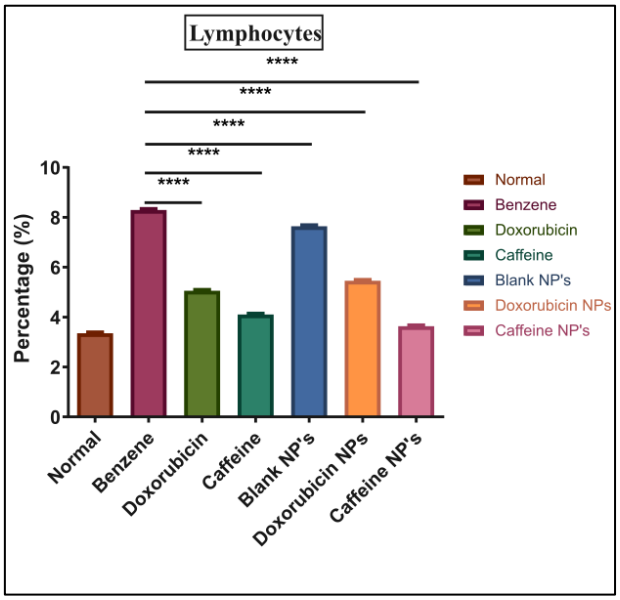

Figure 32 Comparison of Lymphocytes count in different experimental groups

agent exhibited much reduced levels of lymohocytes count resembling control group. Such an effect was not observed in Blank nanoparticles, however lymphocytes count was significantly reduced to normal when treated with caffeine nanoparticles.

4.4.7 Platelets

It was observed by complete blood count that the platelet count was decreased significantly in benzene treated rats as compare to normal. However, Group 3 and 4 having Doxorubicin and Caffeine treated rats respectively, increased platelet count significantly. Such restoration was not observed in Group 5 i.e. Nanomedicine treated rats specially Group 7, instead showed more significant results as compared to free drugs as shown in figure.

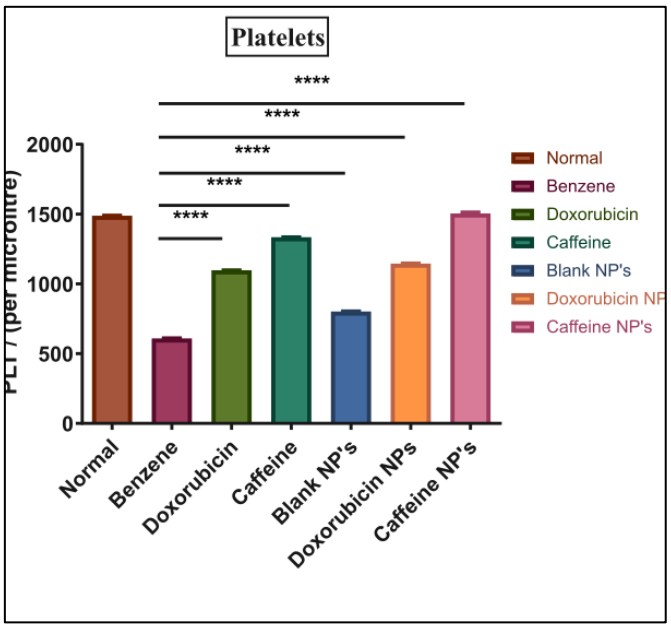

Figure 33 Comparison of Platelets count in different experimental groups

4.4.8 Hemoglobin

It was observed by complete blood count that the hemoglobin level was decreased significantly in benzene treated rats as compare to normal. However, Group 3 and 4 having Doxorubicin and Caffeine treated rats respectively, increased hemoglobin level significantly. Such restoration was not observed in Group 5 i.e. Nanomedicine treated rats specially Group 7, instead showed more significant results as compared to free drugs as shown in figure.

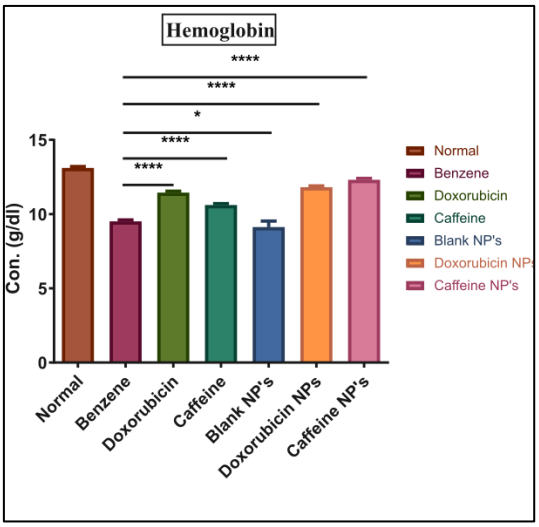

Figure 34 Comparison of Hemoglobin in different experimental groups

4.5 Morphological Analysis

The blood smear slides examination depicted increased number of myeloblasts with immature chromatin and cytoplasmic granules in case of diseased group showing the reminiscent of acute myeloid leukemia. However, with treatment the cells showed improved morphology, the treatment with liposomal nanoparticles depicted better results having normal cell morphology as shown in figure.

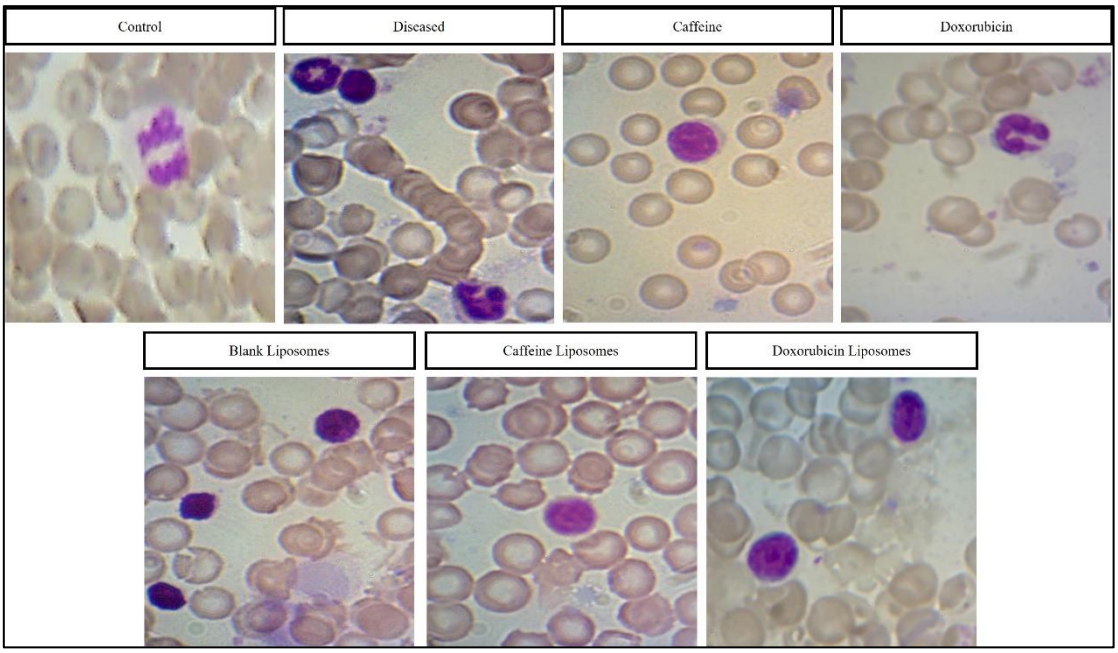

Figure 35 Blood Morphology in different experimental groups

4.6 Histopathological Analysis

4.6.1 Histopathology of Liver

The liver from control group showed normal morphology i.e having normal hepatocytes and portal tracts. In the diseased group, necrosis of hepatocytes, disintegration of plasma membrane, protrusion of cytoplasm along with extramedullary hematopoiesis was observed. Treatment groups showed, normal cell integrity with no infiltration and necrosis. The results of liposomal nanoparticles were more significant.

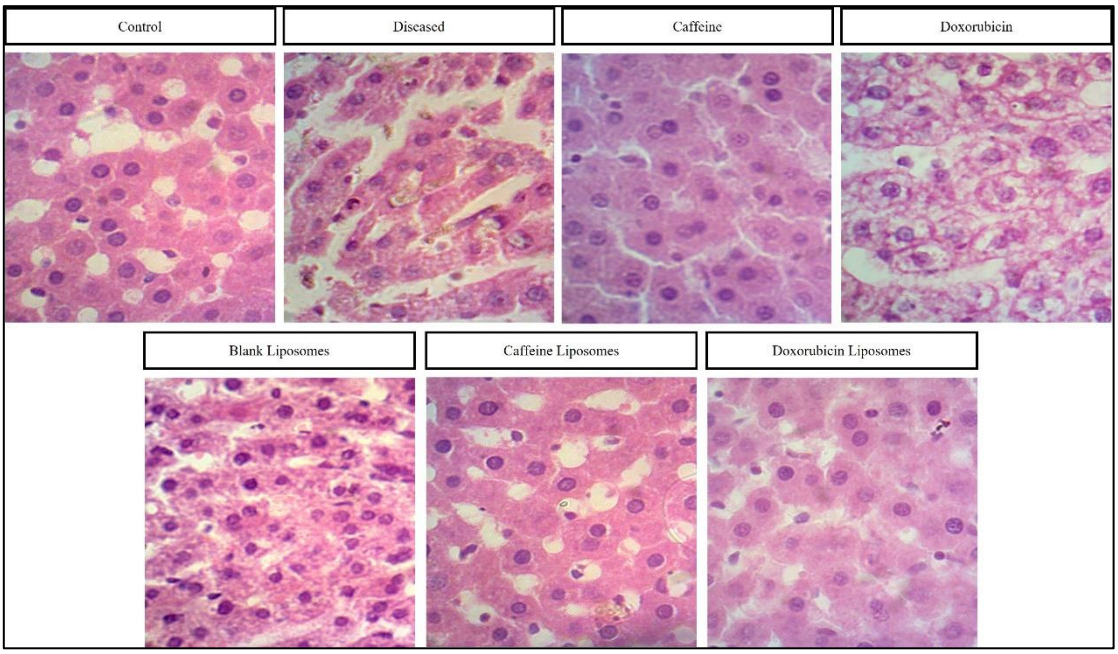

Figure 36 Liver Histology in different experimental groups

4.6.2 Histopathology of Kidney

Control group showed intact structure with normal glomerulus, proximal tubule, and distal tubule. However, diseased group exhibited dilation, inflammation, tubular necrosis, hypertrophy of glomerulus and large space of Bowman's capsule. Analysis of treatment groups showed reduced inflammation, and normal glomerulus. Liposomal groups showed more improved results in comparison to free drug.

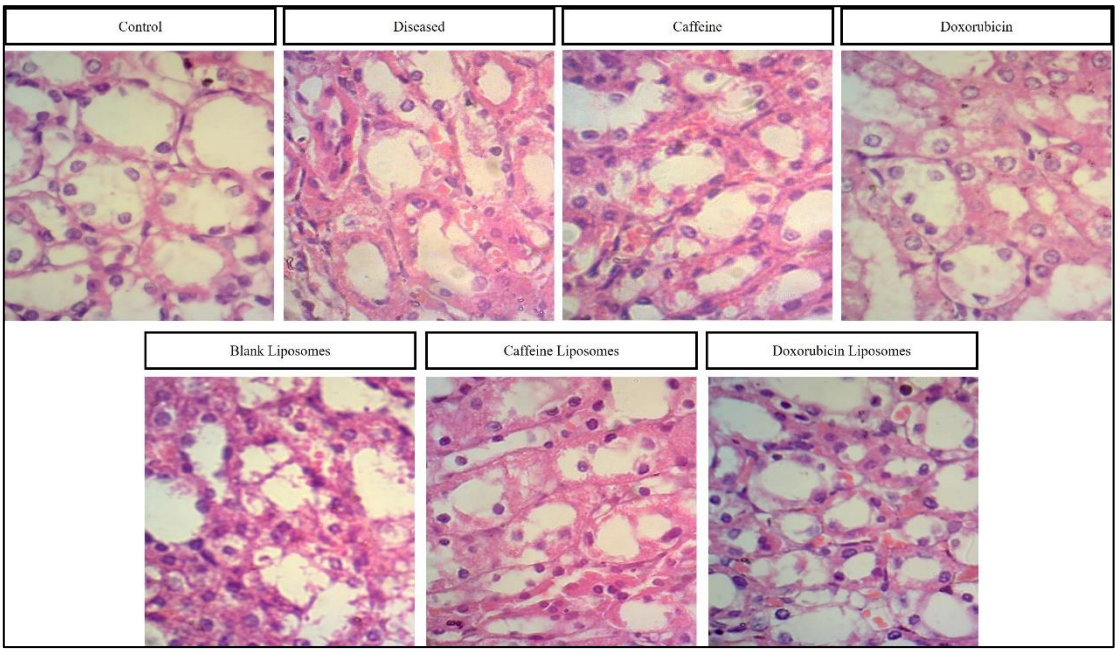

Figure 37 Kidney Histology in different experimental groups

4.6.3 Histopathology of Heart

The control group showed normal cardiac muscles arrangement with no necrosis, infiltration, and inflammation. Infiltration of mononuclear cells was observed in diseased group along with disarrangement of cardiac tissues and inflammation. The Dox treated group showed haemorrhage, necrosis, cellular infiltration. Other treatment groups restore the cardiac structure and show improvement in histopathological results. The liposomal nanoparticles results were more significant.

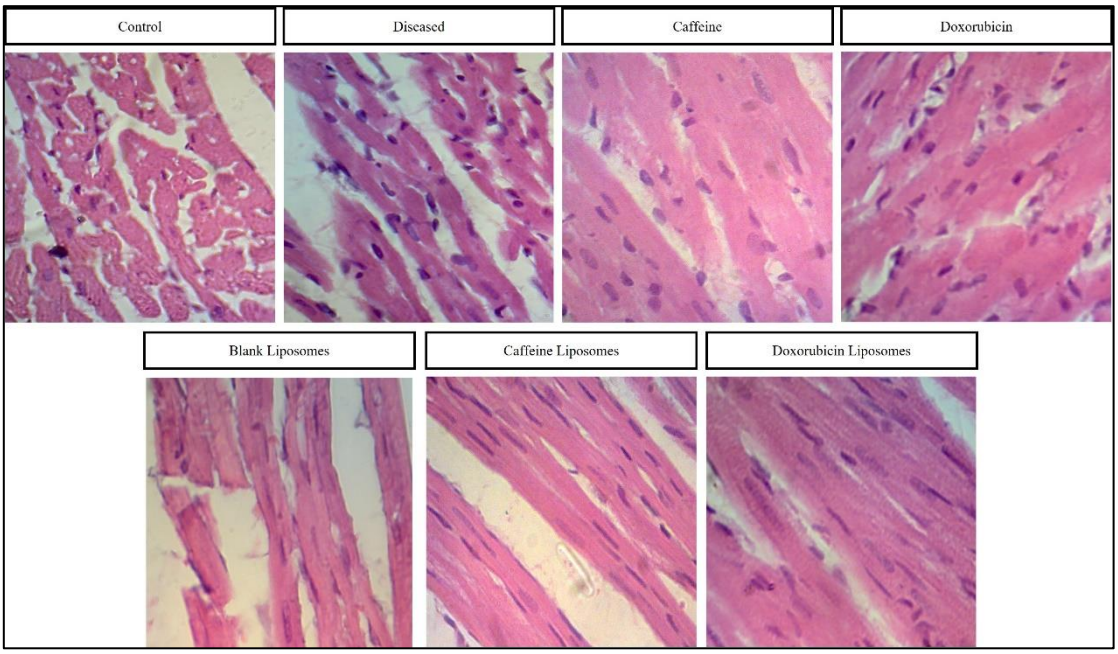

Figure 38 Heart Histology in different experimental groups

s

Chapter 5: Discussion

The global population surge is leading to the emergence of complex health conditions. Traditional therapies are becoming less effective due to growing drug resistance and their inability to combat emerging diseases. Standard chemotherapy treatments have proven to be less effective against cancer because of multidrug resistance and numerous side effects that severely impact quality of life (Housman et al., 2014). Cancer continues to pose a significant health threat with high mortality and morbidity rates worldwide (Hanna et al., 2020). There is a pressing need for innovative therapeutic strategies that offer fewer side effects and enhanced efficacy to address the evolving challenges in leukemia treatment. These challenges underscore the potential for utilizing drug delivery systems that can act as broad-spectrum therapeutic agents in the future (Masood, 2016).

Liposomal nanoparticles are promising drug carriers for treating Acute Myeloid Leukemia (AML) due to their targeted delivery, reduced toxicity, improved stability, and decreased drug resistance (Basha et al., 2014). Caffeine, a well-known stimulant, has shown potential in modulating various signaling pathways involved in cancer cell regulation. Its mechanism of action in cancer cells is multifaceted; it has been observed to interfere with cell cycle progression, primarily by inhibiting the activity of cyclin-dependent kinases (CDKs) and thus inducing cell cycle arrest at the G0/G1 phase, which can lead to apoptosis in tumor cells (Asaad et al., 2004). Higher concentrations of caffeine have been reported to enhance the efficacy of certain chemotherapy drugs, suggesting a synergistic potential in cancer treatment (Friedman et al., 2006). However, the cytotoxic effects of caffeine at elevated concentrations have also been documented, necessitating careful control of dosage to avoid cellular resistance and non-specific toxicity (Kamal et al., 2012). Despite these concerns, caffeine's role as a modulator of cancer cell growth and its potential application in anticancer therapy continues to be an area of active research.

Liposomal nanoparticles of caffeine are created using the thin film hydration method and subsequently coated with PEG 100 to enhance the drug's internalization (Li et al., 2012). The goal of caffeine liposomal nanoparticles is to treat AML in benzene-induced leukemic rats. To confirm the induction of leukemia by benzene, leukemic rats were compared with untreated control rats. A significant rise in blast cells and fragmented red blood cells was observed in the benzene-induced leukemic rats upon Giemsa staining of blood smear slides. Doxorubicin is employed as a reference drug. For free drug caffeine, free doxorubicin is considered as a reference, and for liposomal caffeine nanoparticles, doxorubicin liposomes are regarded as a reference.

The liposomes containing caffeine and doxorubicin were prepared by dissolving the drugs in an appropriate solvent, followed by sonication to form nano-sized particles. Both caffeine and doxorubicin are hydrophilic and are encapsulated within the liposomal vesicle pocket. Nanoparticle size measurements indicated smaller dimensions for the blank liposomes and larger sizes for the drug-loaded liposomes. Zeta potential measurements showed values of -2.6, -7.26, and -5.6 for the blank liposomes, doxorubicin and caffeine nanoparticles, respectively. Over a 16-hour monitoring period, 79% and 74% of the drugs were released from the doxorubicin and caffeine nanoparticles, respectively. FTIR analysis confirmed the presence of distinct functional groups in the liposomal components, drug-loaded liposomes, and blank liposomes, as evidenced by changes in peak intensities.

In vitro assessments of the free drug and drug-entrapped liposomal nanoparticles were performed after thorough literature review. Antioxidant and cytotoxicity assays were conducted, including brine shrimp and hemolytic tests for cytotoxicity and TRP, TAC, and DPPH assays for antioxidant activity. The activities of the liposomes as compared to free drugs were in decreased in TRP, TAC and DPPH which means liposomes protect drug from external environment so the drug release at target will be maximum when administered intravenously. The highest concentration of both the free drug and nanoparticles was the same, at 200 millimolar per 10ml. The cytotoxicity assays revealed a 50%

mortality rate induced by caffeine at an 80% concentration, by doxorubicin at 60%, by caffeine liposomes at concentrations exceeding 100%, and by doxorubicin liposomes at 100%. Reducing the concentration through serial dilutions for free drugs and nanoparticles showed a corresponding decrease in cytotoxicity.

In benzene-induced leukemic rats, an increase in both lymphocytes and neutrophils indicated AML. Higher lymphocyte counts during diagnosis are associated with shorter remission and survival rates (Park et al., 2018). Treatment with doxorubicin nanoparticles showed significant effects as a standard cancer therapy but also resulted in high cytotoxicity, which was less in caffeine liposomes as seen in the treated groups. The hematological profile also improved with drug-loaded nanoparticles, with caffeine liposomes showing a more pronounced and substantial response against leukemic pathogenicity.

The biochemical analysis of hepatic markers revealed an increase in ALT, AST, and decrease in ALP levels in the serum of rats treated with benzene, indicative of liver damage (Akinlolu et al., 2018). However, treatment with caffeine liposomes resulted in a considerable restoration in these hepatic markers, similar to the effects seen with doxorubicin liposomes.

In vitro analyses suggest that free drugs are more cytotoxic compared to their liposomal nanoparticle counterparts, indicating the safer profile of nanoparticle-based drug delivery. Animal model results demonstrated that caffeine liposomes are effective against leukemia with anticancer activity comparable to that of doxorubicin liposomes, a well-established antileukemic drug.

Chapter 6: Conclusion

The encapsulation of caffeine and doxorubicin within liposomal nanoparticles was pursued to mitigate the individual limitations of these compounds and to assess their combined therapeutic impact. The objective was to enhance the bioavailability of caffeine and to minimize the side effects, such as cardiotoxicity, which are commonly associated with doxorubicin. By integrating these drugs into liposomal carriers, we aimed to improve drug stability, circulation time, and targeted delivery, thereby reducing adverse systemic effects. The nanoparticle formulation showed promise, with improvements noted in blood cell morphology, hepatic enzyme activity levels, and a decrease in inflammation across various organs, indicating potential anti-leukemic effects when used either as monotherapy or in combination.

The study was structured to address the bioavailability challenges of caffeine and the significant side effects of doxorubicin by incorporating them into liposomal nanoparticles. These nanoparticles were designed to increase their circulation time and stability, ensuring targeted delivery to minimize unwanted side effects. The animal model used in this research serves as a basis for future investigations into disease mechanisms and drug interactions. The liposomal nanoparticles were synthesized using lipids like DMPC and DPPC, which could potentially be substituted with other lipids to enhance drug loading capacity. Different PEGylation strategies could also be explored to achieve better nanoparticle internalization and extended circulation times. Future research should continue to explore the intricacies of leukemia treatment and the nuanced effects of these drug-loaded nanoparticles. The pathways playing crucial role in AML could also be investigated against these nanoparticles formulation of caffeine.

Chapter 7: References

Abdel Moneim, A., Ezzat, A., Salem, F. E. H., Kassab, R., & El-Yamany, N. A. (2023). Protective effect of virgin coconut oil against doxorubicin-mediated hepatotoxicity in rats. *Advances in Basic and Applied Sciences, 1*(1), 46-54.

Ahmed, A., & Tait, S. W. (2020). Targeting immunogenic cell death in cancer. *Molecular oncology, 14*(12), 2994-3006.

Ajaykumar, C. (2020). Overview on the side effects of doxorubicin. *Advances in Precision Medicine Oncology*.

Alavi, M., & Hamidi, M. (2019). Passive and active targeting in cancer therapy by liposomes and lipid nanoparticles. *Drug metabolism and personalized therapy*, *34*(1), 20180032.

Allen, T. M., & Cullis, P. R. (2004). Drug delivery systems: entering the mainstream. *Science, 303*(5665), 1818-1822.

Anwar, M., Muhammad, F., Akhtar, B., ur Rehman, S., & Saleemi, M. K. (2020). Nephroprotective effects of curcumin loaded chitosan nanoparticles in cypermethrin induced renal toxicity in rabbits. *Environmental Science and Pollution Research, 27*, 14771-14779.

Behrmann, L., Wellbrock, J., & Fiedler, W. (2018). Acute myeloid leukemia and the bone marrow niche—take a closer look. *Frontiers in oncology, 8*, 444.

Blackburn, L. M., Bender, S., & Brown, S. (2019). *Acute leukemia: diagnosis and treatment.* Paper presented at the Seminars in oncology nursing.

Bodley, A., Liu, L. F., Israel, M., Seshadri, R., Koseki, Y., Giuliani, F. C., . . . Potmesil, M. (1989). DNA topoisomerase II-mediated interaction of doxorubicin and daunorubicin congeners with DNA. *Cancer research, 49*(21), 5969-5978.

Boice Jr, J., Storm, H., Curtis, R., Jensen, O., Kleinerman, R., Jensen, H., . . . Fraumeni Jr, J. (1985). Introduction to the study of multiple primary cancers. *National Cancer Institute Monograph, 68*, 3-9.

Calvo, I. A., Gabrielli, N., Iglesias-Baena, I., García-Santamarina, S., Hoe, K.-L., Kim, D. U., . . . Ayté, J. (2009). Genome-wide screen of genes required for caffeine tolerance in fission yeast. *PloS one, 4*(8), e6619.

Caon, I., Bartolini, B., Parnigoni, A., Caravà, E., Moretto, P., Viola, M., . . . Passi, A. (2020). *Revisiting the hallmarks of cancer: The role of hyaluronan.* Paper presented at the Seminars in cancer biology.

Chopra, M., & Bohlander, S. K. (2019). The cell of origin and the leukemia stem cell in acute myeloid leukemia. *Genes, Chromosomes and Cancer*, *58*(12), 850-858.

Clogston, J. D., & Patri, A. K. (2011). Zeta potential measurement. *Characterization of nanoparticles intended for drug delivery*, 63-70.

Daraee, H., Etemadi, A., Kouhi, M., Alimirzalu, S., & Akbarzadeh, A. (2016). Application of liposomes in medicine and drug delivery. *Artificial cells, nanomedicine, and biotechnology, 44*(1), 381-391.

De Jong, W. H., & Borm, P. J. (2008). Drug delivery and nanoparticles: applications and hazards. *International Journal of Nanomedicine, 3*(2), 133-149.

Döhner, H., Estey, E., Grimwade, D., Amadori, S., Appelbaum, F. R., Büchner, T., . . . Larson, R. A. (2017). Diagnosis and management of AML in adults: 2017 ELN recommendations from an international expert panel. *Blood, The Journal of the American Society of Hematology, 129*(4), 424-447.

Fares, J., Fares, M. Y., Khachfe, H. H., Salhab, H. A., & Fares, Y. (2020). Molecular principles of metastasis: a hallmark of cancer revisited. *Signal transduction and targeted therapy, 5*(1), 28.

Farooq, A., Iqbal, A., Rana, N. F., Fatima, M., Maryam, T., Batool, F., . . . Nawaz, A. (2022). A Novel Sprague-Dawley Rat Model Presents Improved NASH/NAFLD Symptoms with PEG Coated Vitexin Liposomes. *International Journal of Molecular Sciences, 23*(6), 3131.

Fouad, Y. A., & Aanei, C. (2017). Revisiting the hallmarks of cancer. *American journal of cancer research, 7*(5), 1016.

Haley, B., & Frenkel, E. (2008). *Nanoparticles for drug delivery in cancer treatment.* Paper presented at the Urologic Oncology: Seminars and original investigations.

Hallek, M., Shanafelt, T. D., & Eichhorst, B. (2018). Chronic lymphocytic leukaemia. *The Lancet, 391*(10129), 1524-1537.

Hanahan, D., & Weinberg, R. A. (2000). The hallmarks of cancer. *cell, 100*(1), 57-70.

Hanahan, D., & Weinberg, R. A. (2011). Hallmarks of cancer: the next generation. *cell, 144*(5), 646-674.

Hassanpour, S. H., & Dehghani, M. (2017). Review of cancer from perspective of molecular. *Journal of cancer research and practice, 4*(4), 127-129.

Hilmer, S. N., Cogger, V. C., Muller, M., & Le Couteur, D. G. (2004). The hepatic pharmacokinetics of doxorubicin and liposomal doxorubicin. *Drug metabolism and disposition, 32*(8), 794-799.

Iqbal, M., Dubey, K., Anwer, T., Ashish, A., & Pillai, K. K. (2008). Protective effects of telmisartan against acute doxorubicin-induced cardiotoxicity in rats. *Pharmacological reports, 60*(3), 382.

Issa, H., Swart, L. E., Rasouli, M., Ashtiani, M., Nakjang, S., Jyotsana, N., . . . Heidenreich, O. (2023). Nanoparticle-mediated targeting of the fusion gene RUNX1/ETO in t (8; 21)-positive acute myeloid leukaemia. *Leukemia, 37*(4), 820-834.

Joshi, M., Bhattacharyya, A., & Ali, S. W. (2008). Characterization techniques for nanotechnology applications in textiles.

Karalexi, M. A., Dessypris, N., Clavel, J., Metayer, C., Erdmann, F., Orsi, L., . . . Greenop, K. R. (2019). Coffee and tea consumption during pregnancy and risk of childhood acute myeloid leukemia: a Childhood Leukemia International Consortium (CLIC) study. *Cancer Epidemiology, 62*, 101581.

Kolachana, P., Subrahmanyam, V. V., Meyer, K. B., Zhang, L., & Smith, M. T. (1993). Benzene and its phenolic metabolites produce oxidative DNA damage in HL60 cells in vitro and in the bone marrow in vivo. *Cancer research, 53*(5), 1023-1026.

Kumari, S., Badana, A. K., & Malla, R. (2018). Reactive oxygen species: a key constituent in cancer survival. *Biomarker insights, 13*, 1177271918755391.

Ladines-Castro, W., Barragán-Ibañez, G., Luna-Pérez, M., Santoyo-Sánchez, A., Collazo-Jaloma, J., Mendoza-García, E., & Ramos-Peñafiel, C. (2016). Morphology of leukaemias. *Revista Médica del Hospital General de México, 79*(2), 107-113.

Lammers, T., Kiessling, F., Hennink, W. E., & Storm, G. (2020). Drug targeting to tumors: principles, pitfalls and (pre-) clinical progress. *Nano-Enabled Medical Applications*, 159-203.

Lu, P. C., Shahbaz, S., & Winn, L. M. (2020). Benzene and its effects on cell signaling pathways related to hematopoiesis and leukemia. *Journal of Applied Toxicology, 40*(8), 1018-1032.

McCafferty, J., Griffiths, A. D., Winter, G., & Chiswell, D. J. (1990). Phage antibodies: filamentous phage displaying antibody variable domains. *Nature, 348*(6301), 552-554.

Meek, M. B., & Klaunig, J. E. (2010). Proposed mode of action of benzene-induced leukemia: Interpreting available data and identifying critical data gaps for risk assessment. *Chemico-biological interactions, 184*(1-2), 279-285.

Misiak, P., Niemirowicz-Laskowska, K., Markiewicz, K. H., Misztalewska-Turkowicz, I., Wielgat, P., Kurowska, I., . . . Wilczewska, A. Z. (2020). Evaluation of cytotoxic effect of cholesterol

End-capped Poly (N-isopropylacrylamide) s on selected normal and neoplastic cells. *International Journal of Nanomedicine*, 7263-7278.

Peng, C., & Ng, J. (2016). The role of epigenetic changes in benzene-induced acute myeloid leukaemia. *J. Clin. Epigenet, 2*(2), 11.

Powers, D., & Nosoudi, N. (2019). Liposomes; from synthesis to targeting macrophages. *Biomedical Research, 30*(2), 288-295.

Roychoudhury, S., Kumar, A., Bhatkar, D., & Sharma, N. K. (2020). Molecular avenues in targeted doxorubicin cancer therapy. *Future Oncology, 16*(11), 687-700.

Schirrmacher, V. (2019). From chemotherapy to biological therapy: A review of novel concepts to reduce the side effects of systemic cancer treatment. *International journal of oncology, 54*(2), 407-419.

Sell, S. (2006). Cancer stem cells and differentiation therapy. *Tumor Biology, 27*(2), 59-70.

Shallis, R. M., Wang, R., Davidoff, A., Ma, X., & Zeidan, A. M. (2019). Epidemiology of acute myeloid leukemia: Recent progress and enduring challenges. *Blood reviews, 36*, 70-87.

Singh, S., Sharma, B., Kanwar, S. S., & Kumar, A. (2016). Lead phytochemicals for anticancer drug development. *Frontiers in plant science, 7*, 1667.

Sive, J. I., & Göttgens, B. (2014). Transcriptional network control of normal and leukaemic haematopoiesis. *Experimental cell research, 329*(2), 255-264.

Stiufiuc, R., Iacovita, C., Nicoara, R., Stiufiuc, G., Florea, A., Achim, M., & Lucaciu, C. M. (2013). One-step synthesis of PEGylated gold nanoparticles with tunable surface charge. *Journal of Nanomaterials, 2013*, 88-88.

Suhail, Y., Cain, M. P., Vanaja, K., Kurywchak, P. A., Levchenko, A., & Kalluri, R. (2019). Systems biology of cancer metastasis. *Cell systems, 9*(2), 109-127.

Sung, H., Ferlay, J., Siegel, R. L., Laversanne, M., Soerjomataram, I., Jemal, A., & Bray, F. (2021). Global cancer statistics 2020: GLOBOCAN estimates of incidence and mortality worldwide for 36 cancers in 185 countries. *CA: a cancer journal for clinicians, 71*(3), 209-249.

Tacar, O., Sriamornsak, P., & Dass, C. R. (2013). Doxorubicin: an update on anticancer molecular action, toxicity and novel drug delivery systems. *Journal of pharmacy and pharmacology, 65*(2), 157-170.

Taha, M., Hassan, M., Essa, S., & Tartor, Y. (2013). Use of Fourier transform infrared spectroscopy (FTIR) spectroscopy for rapid and accurate identification of Yeasts isolated from human and animals. *International journal of veterinary science and medicine, 1*(1), 15-20.

Takami, A. (2018). Hematopoietic stem cell transplantation for acute myeloid leukemia. *International journal of hematology, 107*(5), 513-518.

Terwilliger, T., & Abdul-Hay, M. (2017). Acute lymphoblastic leukemia: a comprehensive review and 2017 update. *Blood cancer journal, 7*(6), e577-e577.

van der Zanden, S. Y., Qiao, X., & Neefjes, J. (2021). New insights into the activities and toxicities of the old anticancer drug doxorubicin. *The FEBS journal, 288*(21), 6095-6111.

Wu, C. (2014). An important player in brine shrimp lethality bioassay: The solvent. *Journal of advanced pharmaceutical technology & research, 5*(1), 57.

Wu, S., Powers, S., Zhu, W., & Hannun, Y. A. (2016). Substantial contribution of extrinsic risk factors to cancer development. *Nature, 529*(7584), 43-47.

Wu, S., Zhu, W., Thompson, P., & Hannun, Y. A. (2018). Evaluating intrinsic and non-intrinsic cancer risk factors. *Nature communications, 9*(1), 3490.

Xiao, Y., Liu, Q., Clulow, A. J., Li, T., Manohar, M., Gilbert, E. P., . . . Boyd, B. J. (2019). PEGylation and surface functionalization of liposomes containing drug nanocrystals for cell-targeted delivery. *Colloids and Surfaces B: Biointerfaces, 182*, 110362.

Yau, A., Lee, J., & Chen, Y. (2021). Nanomaterials for protein delivery in anticancer applications. *Pharmaceutics*, *13*(2), 155.

Yusuf, A., Almotairy, A. R. Z., Henidi, H., Alshehri, O. Y., & Aldughaim, M. S. (2023). Nanoparticles as Drug Delivery Systems: A Review of the Implication of Nanoparticles’ Physicochemical Properties on Responses in Biological Systems. *Polymers*, *15*(7), 1596. Retrieved from https://www.mdpi.com/2073-4360/15/7/1596

Zhang, Q., Yang, Q., Weng, Y., Huang, Z., Chen, R., Zhu, Y., . . . Yu, K. (2021). Neutrophil-to-lymphocyte ratio correlates with prognosis and response to chemotherapy in patients with non-M3 de novo acute myeloid leukemia. *Translational Cancer Research*, *10*(2), 1013.